OCCURRENCE AND MINERAL CHEMISTRY OF HIGH PRESSURE PHASES, POTRILLO BASALT, SOUTHCENTRAL NEW MEXICO

Final

Technical Report

Principal Investigator: J. M. Hoffer

Period Covered: June 1, 1980 to May 31, 1982

Name of Institution: The University of Texas at El Paso

Grant Number: NASA NSG 9062

May 31, 1982

This Report

Represents an M.S. Thesis

by

Tatum Michael Sheffield

Department of Geological Sciences

The University of Texas at El Paso

El Paso, Texas 79968

Thesis Director

Dr. J. M. Hoffer

ACKNOWLEDGEMENTS

I wish to thank Dr. Jerry M. Hoffer, University of Texas at El Paso, who suggested the project and guided me throughout the course of the work. The thesis was financed through a grant to Dr. Jerry M. Hoffer from the National Aeronautics and Space Administration (Grant NSG 9062). Special thanks are due also to Dr. D. Barker, University of Texas at El Paso, for supplying the listing of the CIPW Norm Program. I also wish to thank my friends and colleagues at the University of Texas at El Paso for their constant help and many discussions.

ABSTRACT

The area of investigation is located in the southwestern corner of Dona Ana County, New Mexico. The West Potrillo Basalt Field is a broad, north-trending range composed of numerous Quaternary basalt flows and cinder cones.

Most of the flows are alkali-olivine basalts with rare occurrences of flows with a tholeiitic composition. The basalts are vesicular, hypocrystalline, microporphyritic to porphyritic. Feldspar megacrysts are found on the flanks of cinder cones, as inclusions within lava flows and in the cores of volcanic bombs. Based on petrography and chemistry, the phenocrysts are interpreted to have formed at great depth rather than as phenocrysts of larger crystal aggregates.

Hoffer (1976) divided the basalts into two members: Member 1, an older plagioclase-rich basalt; and Member 2, a younger olivine-rich basalt. The presence of these two members have been confirmed by modal and chemical analysis. Chemical analysis has also confirmed the presence of flows that are tholeiitic in composition and could be remnants of an original tholeiitic parent magma. Eruptions from different levels of a differentiated magma chamber are proposed to account for the two members.

TABLE OF CONTENTS

LIST OF FIGURES

LIST OF PLATES

LIST OF TABLES

INTRODUCTION

The West Potrillo Basalt Field is located in the southwestern corner of Dona Ana County, New Mexico, approximately 48 km west of El Paso, Texas. The West Potrillos Mountains are bounded on the south by the boundary between the United States and Mexico, on the east by longitude 107°15'W, on the north by latitude 32°13'N, and on the west by longitude 107°15'W (Fig. 1).

The southern West Potrillo Mountains are accessible by traveling on Interstate 10 to the Mesa Street Exit, then traveling west on Mesa Street to Country Club Road. Turn right on McNutt Road and travel west onto the LaMesa surface 4.8 km and bear right through Strauss, New Mexico. Turn left at the Columbus Road to Mt. Riley and Columbus, New Mexico. Travel west for about 32 km approximately paralleling the international border. Access to the southern West Potrillo is from ranch roads north of the Columbus Road. The northern West Potrillo is easily accessible by traveling west on Interstate 10 from El Paso to Las Cruces, then continue past Las Cruces for 40 km. Access to the northern West Potrillos is by ranch roads south of Interstate 10.

Previous Work

Previous work in the area was done by Hoffer (1973) who described the geology and petrology of the area. Renault (1970) analyzed and reported the major element geochemistry of

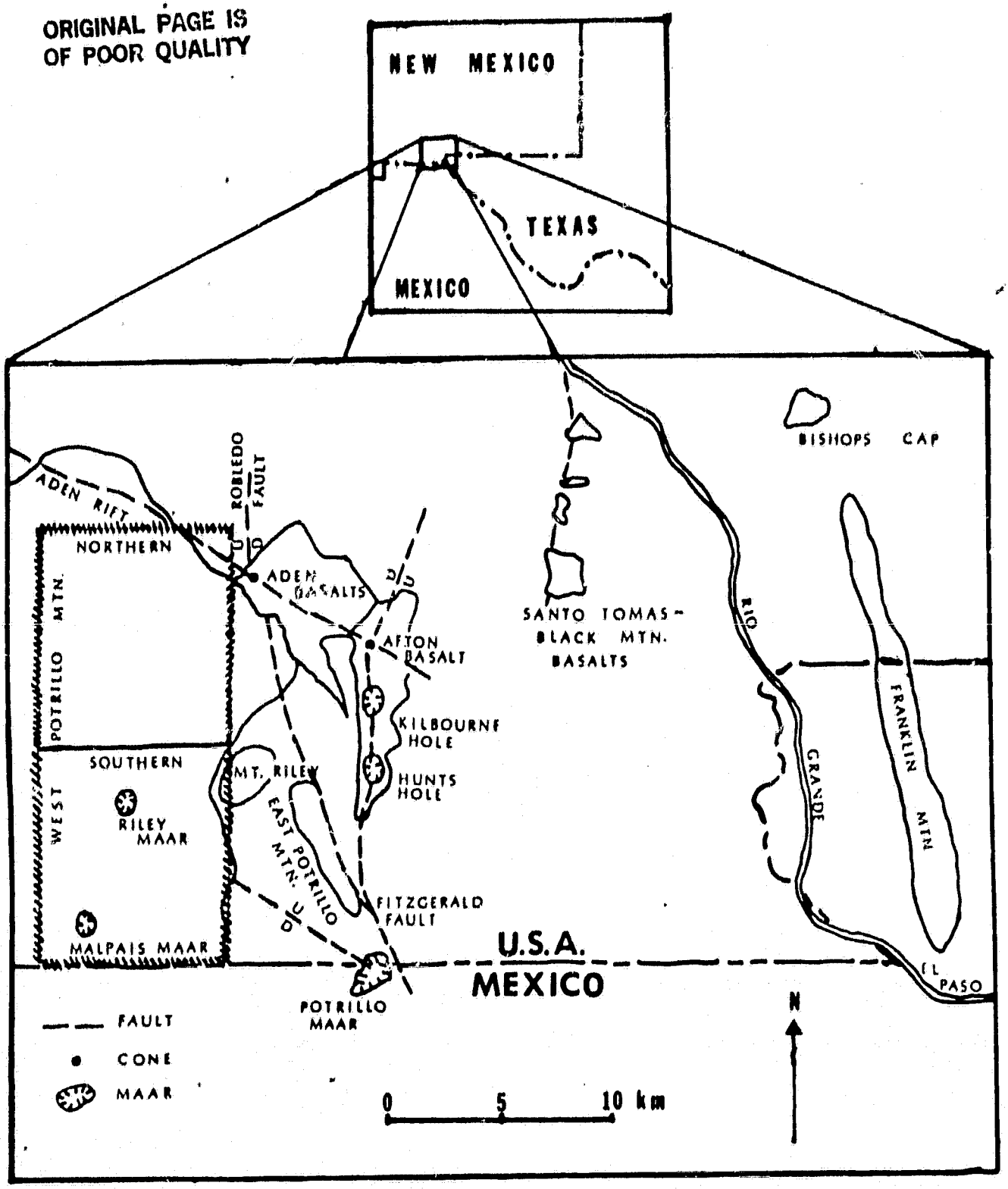

Fig. 1. Index map of the Potrillo Basalt Field, study area shown in hatchers.

a selected number of basalts from the West Potrillo Mountains. Hoffer (1976) discussed the regional geology and petrology of the basalt in relation to the Rio Grande Rift. Hoffer and Hoffer (1973) discussed the composition and structural state of feldspar inclusions from alkali-olivine basalts in the West Potrillo Basalts. Bersch (1977) reported on the petrography and geology of the southern West Potrillo Basalt Field, and Ortiz (1979) described the megacrysts and mafic and ultramafic inclusions of the southern West Potrillo Basalt Field.

Purpose

The purpose of this thesis is to: 1) determine the major element chemistry of the entire West Potrillo Basalt field, 2) describe the mineralogy and textures of the basalts, and 3) determine the relationships between the feldspar megacrysts and the host basalt.

Geography and Physiography

The Potrillo Volcanic field can be divided into three regions: 1) a region to the east composed of the Santo Tomas-Black Mountain basalt field; 2) a central region containing the Aden Afton basalts and several maars (Kilbourne Hole, Hunts Hole, and Potrillo maar); and 3) the region of the West Potrillo Mountains (Hoffer, 1976).

The Potrillo basalt flows were erupted onto the LaMesa surface, a flat plain developed within the Mesilla Bolson during

middle to late Pleistocene (Hawley and Kottlowski, 1969). The West Potrillo Mountains, the area of this investigation, forms a broad, north-trending constructional plateau composed of numerous basalt flows and over 160 cinder cones. The area is included in the Mexican highland section of the Basin and Range province (Fenneman, 1931).

Vegetation and Climate

The area is covered with cholla, mesquite bush, narrow leaf yucca, prickly pear, lechugilla, and barrel cacti.

The climate of the study area is semi-arid. Average summer temperatures frequently exceed 100°F (38°C); winter daytime temperatures are seldom less than 32°F (0°C).

The average yearly precipitation is nine inches (23 cm), most of which occurs as thunderstorms in July and August (U.S.D.A., 1941).

Prevailing winds on the surface are westerly averaging about 9.6 km per hour. During the spring months the wind velocity averages 40 km per hour (King et al., 1969).

Field and Laboratory Work

Collection of Samples

Sampling of the northern West Potrillo Basalt was done during the summer of 1979 by the author. Samples were collected of basalt flows, cinder cones, volcanic bombs, and feldspar megacrysts. Samples from the southern West Potrillo, collected by

Michael Bersch and Terry Ortiz, were also utilized in this study. A total of 1010 samples were collected -- 162 of basalt, and 848 feldspar megacrysts. Basalt and feldspar megacrysts sample locations are shown in Appendix B.

Preparation of Samples

The samples were prepared and analyzed during the summer and fall of 1980. One hundred and sixty-seven samples were ground in a disc grinder, pulverized in a SPEX 8500 shatterbox for six minutes and pellitized under 20 tons of pressure in a Spex-25 hydraulic press. Of this total, 77 samples were from basalt flows, 18 from cinder cones, 19 samples of altered basalt, 2 volcanic bombs, 1 basalt dike, and 50 feldspar megacrysts. Also, 20 thin sections were prepared; 15 were from flow basalts and 5 from volcanic bombs.

Methods of Analysis

Petrography

Fifteen thin sections were observed under a standard petrographic microscope. Observations were made for texture and major mineral constituents with estimates of mineral composition were possible. Point coints based on 100 points were completed on 10 thin sections.

X-ray Fluorescence

One hundred and sixty-six samples were analyzed on an Ortec TEFA Model 6110 X-Ray energy dispersive fluorescence analyzer. Analyses were made for the ten major oxides: SiO_2, TiO_2,

Al_2O_3, FeO, MnO, MgO, CaO, Na_2O, K_2O, and P_2O_5. The standard CALC program was used for calculating intensities and concentrations of X-ray lines in combination with the FLINT inter-element correction protocal to determine matrix corrections for the samples.

Norm Calculations

A standard CIPW norm program was obtained from the University of Texas at Austin and adapted to the University of Texas at El Paso's IBM 360 computer by the author.

CIPW Norms were calculated for 77 basalt samples from the chemical analysis obtained by x-ray fluorescence. The norm notation used here is listed in Table 1.

Three adjustments were made to the oxide percentages before CIPW norms were calculated:

1) Total iron was recorded as FeO from x-ray fluorescence data. For the purposes of calculating molecular norms, the FeO was separated into FeO and Fe_2O_3 using a ratio of 1.8 to 1. This ratio was based on chemical analysis of ferrous and ferric iron by T. Asari, Japan Analytical Laboratory, of two samples from the West Potrillo Basalt Field (Hoffer, 1976).

2) An upper limit on Fe_2O_3 was set using the equation based on Irvine and Barager (1971):

$$\%Fe_2O_3 = \%TiO_2 + 1.5$$

Table 1. Norm Symbols

Q - quartz, SiO_2

C - corundum, Al_2O_3

Or - orthoclase, $KAlSi_3O_8$

Ab - albite, $NaAlSi_3O_8$

An - anorthite, $CaAl_2Si_2O_8$

Lc - leucite, $KAlSi_2O_6$

Ne - nepheline, $NaAlSi_2O_4$

Di - diopside = wollastonite(Wo) + enstatite(En) + ferrosilite(Fs)
= $CaSiO_3$ + $MgSiO_3$ + $FeSiO_3$

Hy - hypersthene = En + Fs = $MgSiO_3$ + $FeSiO_3$

Ol - olivine = Fo + Fa = Mg_2SiO_4 + Fe_2SiO_4

Mt - magnetite, Fe_3O_4

Il - ilmenite, $FeTiO_3$

Ap - apatite, $Ca_5(PO_4)_3$

Cc - calcite, $CaCO_3$

Ab'- Ab + 5/3Ne @

Plagioclase = Ab + An

Normative plagioclase composition = 100 * An/An + Ab + 5/3Ne

Normative color index = 100 - (Q + Or + Ab + An + Lc + Ne)

@ Note: Ne is converted to Ab based on the relation:

$$NaAlSiO_4 + 2SiO_2 = NaAlSi_3O_8$$

$$3Ne + 2Q = 5Ab$$

So each unit of Ne gives 5/3 units of Ab.

No change occurs if the analysis value is less, but an excess is converted to FeO, and yields a more undersaturated norm.

3) In order to place all comparisons on the same basis, the oxide analysis was recalculated to 100% without CO_2.

The above adjustments assume that the rock was exposed to volatiles only during metamorphism or alteration.

The computer program outputs both weight, percent and molecular norms. For purposes of graphical projection, the molecular norm values were used with Ne recast as Ab (Table 1). This allows the ratio of Ab to Or to be a more accurate measure of the atomic ratio of sodium to potassium (Irvine and Barager, 1971).

REGIONAL GEOLOGY

Geologic History

The West Potrillo Basalt Field is located in the southern end of the Rio Grande rift (Fig. 2). The boundaries of the southern end of the rift are outlined based on the assumption that high heat flow, young faulting (less than 0.4 m.y.), occurrence of late Pliocene and younger volcanoes, and deep basins are surface expressions of the rifts deep thermal structure (Seager and Morgan, 1979).

Strata ranging from Paleozoic to Holocene are exposed in the area. During late Paleozoic and early Mesozoic repeated advances and withdrawals of seas initiated the deposition of marine sediments. Folding and faulting of lower Cretaceous strata occurred during the Laramide disturbance in the East Potrillo Mountains. Northwest of the East Potrillo Mountains, Mt. Riley-Mt. Cox, a large andesitic pluton was emplaced during early to middle Tertiary. During middle Tertiary, high-angle faulting and uplift occurred in the East Potrillo Mountains and initiated the formation of the Mesilla bolson, an intermontane basin (Hoffer, 1976).

Rifting in the area began about 32 m.y. ago during the middle Tertiary. Basaltic andesite volcanism occurred to about 20 m.y. ago, followed by a lull in magmatism between 20 and 13 m.y. ago. Volcanism along the rift began again after the (20-13 m.y.) lull, with a sharp increase in basaltic volcanism about 5

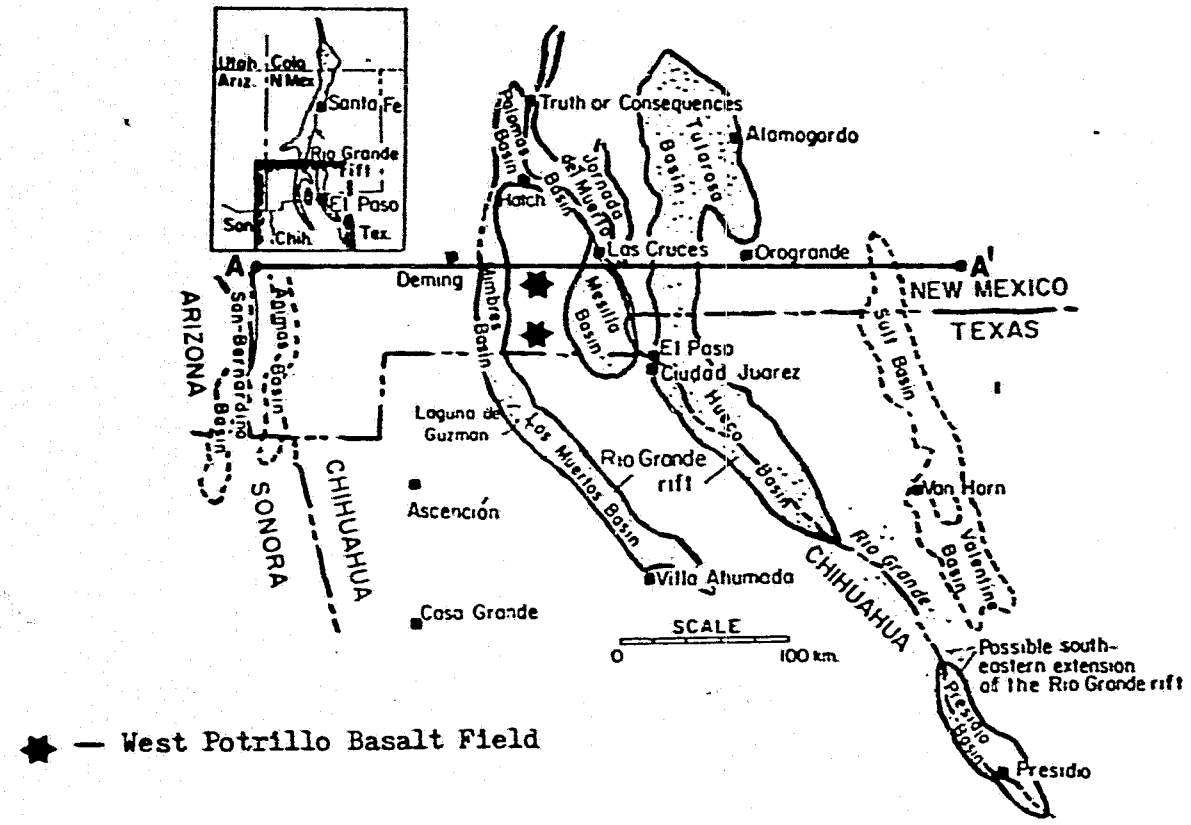

Fig. 2 Location map, southern Rio Grande rift region.
(after Seager and Morgan, 1979)

m.y. ago (Chapin, 1979).

According to Chapin and Seager (1975), the 20-13 m.y. pause in volcanism separates two different thermal regimes -- an older one occurring with initial extension in the rift producing basaltic andesite volcanism, and a younger regime related to critical thinning of the lithosphere beneath the rift, and which generated alkali olivine basalts. The sharp increase in basaltic volcanism 5 m.y. ago is probably a result of the culmination of block faulting 8 to 3 m.y. ago with associated extension of the crust.

Faulting

The study area contains a number of major high-angle faults; the largest being the Robledo and Fitzgerald faults (Fig. 1). The Robeldo fault crops out on the east side of the East Potrillo Mountains along a northwest-trending scarp. The scarp can be traced southward from the East Potrillo Mountains into Mexico and northward under the Aden flows. The fault emerges north of the Aden flows east of Aden crater and trends northeastward into the Robledo Mountains north of Las Cruces, New Mexico (DeHon, 1965). The Fitzgerald fault parallels the Robledo fault to the east and trends southwestward under the Afton flows (Fig. 1).

STRATIGRAPHY

Introduction

The exposed rocks of the study area are Tertiary and Quaternary in age. The Tertiary rocks consist of silicic volcanic rocks and the intrusive bodies of Mt. Riley and Mt. Cox. Rocks of Quaternary age consist of cinder cones, basaltic lava flows, basaltic dikes, and tuffs and tuff-breccia associated with maar volcanoes of the Potrillo Basalt.

Tertiary

Silicic Volcanic Rocks

Silicic volcanic rocks crop out on the west and north flanks of the study area. Hoffer (1976) states that the exact age of these igneous bodies is not known, but since many show intrusive contacts with Cretaceous strata they are considered to be at least Tertiary. The silicic volcanic rocks include tuffs and flow breccias. The tuffs are thinly bedded and contain phenocrysts of plagioclase and orthoclase.

Mt. Riley-Mt. Cox Intrusion

The Mt. Riley-Mt. Cox intrusive mass rises 1600 ft above the La Mesa Surface reaching an elevation of 6000 ft (Hoffer, 1976). The intrusion is a light-gray, holocrystalline, microporphyritic andesite to rhyodacite (Millican, 1971).

Millican (1971) states that chemical and mineralogical similarities of the Mt. Riley-Mt. Cox pluton to intrusive andes-

ites in the El Paso-Juarez area indicates common or similar origins, and are of possible Eocene age.

Quaternary

The basalts of the West Potrillo Mountains are thought to be Quaternary (Hoffer, 1976). The volcanics consist of numerous cinder cones (Plate 1), basaltic tuffs and breccias, maar volcanoes, and thin alkali olivine basalt flows.

Based upon field relationships and petrography, Hoffer (1976) has divided the West Potrillo Basalts into two members: an older plagioclase-rich member, and a younger olivine-rich member. In addition Hoffer (1976) suggested that the cinder cones, based upon shape and degree of dissection, are of two distinct ages: young and old (see Table 2).

Holocene

Sand

Holocene deposits of sand cover large areas of basalt and collect on the east side of many cinder cones as a result of the predominantly westerly winds.

The blown sand is composed primarily of subrounded, clear to iron-coated, quartz grains averaging over 70%. Other minerals identified are feldspar, opaques, zircon, tourmaline, and pyroxene (Hoffer, 1976).

Plate 1 View of West Potrillo cinder cones.

Table 2 Cinder cone characteristics (after Hoffer, 1976)

	Young Cones	Old Cones
Height	200-500 feet	50-300 feet
Slopes	20-25 degrees cut by shallow arroyas	10-20 degrees cut by deep arroyas
Spatter	rare	abundant
Vents	single	multiple
Xenoliths	rare	abundant
Shape	horseshoe in plan	horseshoe to irregular in plan

Alluvium

Recent alluvium occurs in minor playas and in stream channels throughout the study area. Stream channel material is silt to medium-grained sand. At the base of cinder cones the deposits become conglomeratic containing pebbles and cobbles of basalt (Bersch, 1977).

PETROGRAPHY

Introduction

Twenty thin sections from the northern West Potrillo Basalt were examined for mineral composition. Modal percentages were estimated for ten basalt samples, five from Member 1, and five from Member 2. Estimated modal percentages of basalt samples from the northern West Potrillo Basalt are shown in Appendix B. A summary of comparative modal percentages of the two members is given in Table 3.

Potrillo Basalt

Texture

The West Potrillo Basalts are highly vesicular to dense, and ranges in color from dark gray to black. Surface weathering yields a reddish brown to purple color on some flows. The lava flows are hypocrystalline, microporporphyritic to porphyritic with a microcrystalline groundmass. The texture of the groundmass is intersertal to intergranular.

Essential Minerals

Plagioclase Feldspar

Plagioclase occurs mostly in the groundmass as subhedral laths that are aligned and show flow structure around phenocrysts (Plate 2). The laths range from .01 mm to 1 mm long with a composition that ranges from An_{40} to An_{70} (andesite to labra-

Plate 2 Plagioclase flow around phenocrysts.

Table 3

Summary of Average Modal Analysis

	Averages		Averages	
	Member 1	Hoffer*	Member 2	Hoffer*
Plagioclase	27	26	20	19
Clinopyroxene	24	27	37	39
Olivine plus Iddingsite	9	13	12	18
Opaque Minerals	14	14	16	12
Glass	23	20	13	12
Other	3	—	2	—

Samples averaged as Member 1 this study:
065,066,070,072,073,074,075,075a,077,078,080,081,084,085,103,104,105
(from Bersch,1977)
203,245,246,247,270
(Appendix B) Total Samples 22

Samples averaged as Member 2 this study:
015,017,020,024,029,033,037,039,045,047,048,050,052,053,057,058,076,083
(from Bersch,1977)
205,213,215,216,241
(Appendix B) Total Samples 23

* Average modal analysis from Hoffer(1976)

dorite). Average plagioclase lath size in Member 1 and Member 2 is 0.1 and 0.6 mm, respectively. Plagioclase laths in both members show wavy extinction indicating chemical zonation. Pericline, carlsbad and albite twinning are common in both members. Member 1 has a slightly higher modal percentage of plagioclase than Member 2, 27% and 20%, respectively.

Clinopyroxene

Clinopyroxene occurs in the groundmass and as phenocrysts. Bersch (1977) set an arbitrary maximum dimension of 0.3 mm to divide groundmass and phenocrysts of clinopyroxene in the West Potrillo Basalts. Member 1 contains clinopyroxene in the groundmass and as phenocrysts less than 0.5 mm in length, and Member 2 has clinopyroxene phenocrysts 0.3 go 2.5 mm in length (Bersch, 1977). The average modal composition of clinopyroxene in Member 1 and Member 2 is 24% and 37%, respectively. The groundmass clinopyroxene is euhedral, prismatic to equidimensional microlites and ranges in composition from augite to titanium-rich augite. They varied in color from brown to greenish-yellow.

The phenocrysts of titan-augite are the most abundant of the two sizes of clinopyroxene. The phenocrysts are usually light to dark brown. Zoning from light brown centers to dark brown rims is common. The phenocrysts are euhedral with occillatory zoning and hour-glass structure common. Many of the phenocrysts have incomplete or skeletal centers (Plate 3) which could indicate formation during a period of rapid growth (Bersch, 1977).

Olivine

Olivine occurs as euhedral to subhedral, six-sided, prismatic phenocrysts. The crystals range from 0.1 to 6.0 mm in length. The olivine composition, as indicated by a high 2V of 85 to 90°, is Fa_{10} (Bersch, 1977). A high Mg value is supported by the high normative Fo in the norm calculations (Appendix C). Member 2 has a slightly higher modal olivine percentage than Member 1, 12% and 9%, respectively. The olivine phenocrysts in lava flows and volcanic bombs are commonly embayed, indicating that they were not in equilibrium with the magma (Plates 4a and 4b). Inclusions of chrome spinel and opaque minerals are common and could indicate crystallization at depth. Some olivine phenocrysts also exhibit multiple twinning which gives the crystal a saw-tooth appearance.

Replacement of olivine by opaque material occurs in samples from cinder cones or from small flows associated with the cinder cones. Olivine is altered to iddingsite which occurs as thin rims around the olivine. In some samples complete alteration of olivine to iddingsite, hematite and serpentine occurs.

Bersch (1977) suggested that the selective replacement of olivine took place within the vent of the cinder cone, with volatiles streaming through the magma hydrating and oxidizing the olivine. Iddingsite, chlorite and serpentine represent the end state of deuteric alteration.

Plate 3 Titanaugite showing skeletal centers.

Plate 4a Olivine embayed by groundmass in flow.

Plate 4b Olivine embayed by groundmass in volcanic bomb.

Accessory Minerals

Opaque Minerals

Opaque minerals occur in the groundmass of both Members as euhedral, equidimensional grains usually less than 0.6 mm. The most common opaque mineral is magnetite, a steel blue-black mineral that is commonly octahedral. Crystals of illmenite are also found, occurring as violet-black, flake-like crystals.

Analcime

Analcime is present in the groundmass as anhedral patches in cracks, and as a lining in vesicles.

Chrome Spinel

Chrome spinel occurs in olivine phenocrysts of both Member 1 and 2 as brown, euhedral grains less than 0.05 mm.

Glass

Dark brown glass occurs as scattered patches and interstitial material. Some samples show a devitrification of the glass and clinopyroxene microlites in both Member 1 and 2. Member 1 has a higher modal glass percent than Member 2, 23% and 13%, respectively.

Serpentine and Chlorite

Cholorite is found along the rims and cracks of some olivine phenocrysts in both Member 1 and 2. Serpentine occurs in the groundmass as patches and stringers, and in some samples appears after chlorite in the alteration of olivine.

Calcite

Secondary calcite lines and fills the vesicles of many of the flows of both Member 1 and 2.

Feldspar Megacrysts

The alkali and plagioclase feldspar megacrysts are gray to colorless, anhedral to euhedral, ranging in size from 3 mm to 6 cm (Plate 5). A 6 cm feldspar megacryst was reported by Ortiz (1979).

Iron oxide inclusions and iron oxide staining on the surface are present on some of the megacrysts that are found loose on the flanks of some of the cinder cones. Little or no reaction has taken place between the crystals and the basalt; however, feldspar megacrysts included in the volcanic bombs do show some embayment indicating that they were not in equilibrium with the magma (Plate 6).

Twinning lamellae and conchoidal fracture is common with albite and pericline twinning present in many samples. Ortiz (1979) states that the megacrysts show varying intensities of strain shadows that could have developed at depth or as a result of unloading at the surface.

Plate 5 Representative feldspars from West Potrillo basalts.

Plate 6 Feldspar in bomb (embayed).

GEOCHEMISTRY

West Potrillo Basalt

Introduction

Eighty samples of the West Potrillo Basalt field were analyzed for ten major oxides by x-ray fluorescence; analyses are reported in weight percent.

Seventy-seven of the samples represent basalt flows of Member 1 and 2. The results of these analyses are shown in Tables 4, 5, and 6. Normative calculations were also performed for the samples and the results are shown in Appendix C. The samples were classified according to the scheme of Irvine and Baragar (1971). Also, two volcanic bombs and one dike were analyzed with the results shown in Table 6. Locations of the basalt and megacryst samples are given in Appendix A and Plate 7.

Classification

The basalts were classified on the basis of an alkali ($Na_2O + K_2O$) vs silica diagram (Fig. 3). The diagram shows that the majority of the samples plot as basalts but range from basanite (< 5% normative Ne) to basaltic andesite. The samples range from 42 to 47% SiO_2, and contain both normative hypersthene and nepheline. Two of the samples (209, 242; Table 6) plot as basaltic andesite with an average silica content of 54%. The distinction between basalt and basaltic andesites at SiO_2 = 52% is compatible with the terminology of Carmichael et al. (1974).

Table 4

Chemical Compositions

Member 1 in Oxide Percent

Sample	SiO_2	TiO_2	Al_2O_3	FeO*	MnO	MgO	CaO	Na_2O	K_2O	P_2O_5	Total	S.I.
043	45.24	2.78	15.22	12.11	0.16	8.40	10.34	2.82	1.66	0.73	99.46	33.6
065	44.10	2.70	16.10	11.85	0.16	8.38	11.19	2.66	1.65	0.67	99.46	34.1
066	42.19	2.71	13.32	13.02	0.16	8.63	14.14	2.75	1.34	0.68	98.94	33.5
070	44.59	2.73	14.96	12.22	0.15	9.25	10.34	3.21	1.45	0.59	99.49	35.4
072	43.65	1.86	13.96	11.37	0.12	8.54	15.05	2.63	1.64	0.79	99.61	35.3
073	44.02	2.99	14.95	12.97	0.17	8.73	10.55	2.71	1.44	0.70	99.23	33.8
074	45.68	2.77	15.06	13.06	0.15	8.12	8.58	2.71	2.03	0.58	98.74	31.3
078	45.48	2.32	14.59	11.76	0.15	9.30	9.12	3.36	2.12	0.60	98.80	35.0
081	43.83	2.89	14.47	12.78	0.16	9.00	11.00	2.77	1.54	0.70	99.14	34.5
082	43.26	2.72	14.90	14.19	0.18	6.07	12.49	3.28	1.28	0.65	99.02	24.5
084	48.07	2.24	13.96	11.67	0.17	8.88	10.41	2.81	0.75	0.69	99.65	36.8
085	46.65	2.57	14.44	11.73	0.15	9.15	10.54	2.92	0.94	0.55	99.64	36.9
097	45.01	2.97	14.69	13.55	0.17	6.43	11.06	2.77	1.14	0.71	98.50	26.9

Table 4

(Con't)

Sample	SiO_2	TiO_2	Al_2O_3	FeO*	MnO	MgO	CaO	Na_2O	K_2O	P_2O_5	Total	S.I.
103	44.56	2.38	15.90	12.18	0.16	7.24	12.13	2.77	1.45	0.64	99.41	30.6
104	43.38	2.57	15.94	13.00	0.16	7.29	11.82	2.77	1.54	0.62	99.09	29.6
105	44.14	2.31	14.14	12.54	0.16	9.27	11.05	2.66	1.50	0.73	98.50	35.7
202	45.38	2.67	14.16	12.23	0.19	9.92	9.49	2.87	1.54	0.70	99.15	37.4
203	44.65	2.26	12.43	12.86	0.19	10.18	12.65	2.88	0.65	0.61	99.36	38.3
204	44.60	2.60	13.86	12.25	0.18	10.08	10.48	2.87	1.74	0.74	99.40	37.4
218	45.03	2.15	13.86	12.20	0.17	9.56	11.30	2.94	1.67	0.67	99.55	36.3
220	46.20	2.41	14.43	13.05	0.19	8.00	8.85	2.83	2.00	0.64	98.60	30.9
244	47.40	2.16	14.13	12.82	0.20	6.38	10.45	3.32	1.29	0.67	98.82	26.8
246	45.82	2.75	14.42	12.57	0.19	8.86	9.44	2.91	1.09	0.71	98.76	34.8
247	45.79	2.71	14.24	12.71	0.19	8.59	9.60	2.93	1.04	0.73	98.53	34.0
257	46.43	2.79	14.80	12.25	0.19	8.87	9.26	2.90	1.34	0.76	99.59	34.9
258	45.55	2.75	14.31	12.60	0.19	8.91	9.54	2.86	1.31	0.71	98.73	34.8
259	45.73	2.72	14.35	12.32	0.18	9.42	9.53	2.88	1.26	0.67	99.06	36.4
261	45.87	2.77	14.62	12.00	0.19	9.93	9.26	2.89	1.26	0.68	99.47	38.1

Table 4

(Con't)

Sample	SiO_2	TiO_2	Al_2O_3	FeO*	MnO	MgO	CaO	Na_2O	K_2O	P_2O_5	Total	S.I.
270	46.41	2.11	14.37	12.51	0.19	8.96	8.94	2.94	1.84	0.67	98.94	34.1
273	45.50	1.72	13.54	11.50	0.19	9.98	12.15	2.75	1.52	0.65	99.60	38.6
Average	45.14	2.53	14.48	12.46	0.17	8.67	10.69	2.87	1.43	0.67	99.10	34.0
S.D.	1.26	0.31	0.75	0.61	0.01	1.08	1.54	0.18	0.34	0.05		

MgO range = 6.07 to 10.18

S.I. = 100 MgO/(MgO + FeO + K_2O + Na_2O)

Table 5.

Chemical Composition

Member 2 in Oxide Percent

Sample	SiO_2	TiO_2	Al_2O_3	FeO*	MnO	MgO	CaO	Na_2O	K_2O	P_2O_5	Total	S.I.
015	45.19	2.33	15.07	10.97	0.16	9.76	11.16	2.83	1.04	0.64	99.15	39.7
017	45.41	2.67	14.96	11.62	0.16	8.70	11.03	2.74	1.00	0.69	98.98	36.2
018	42.98	2.55	14.13	11.32	0.16	12.46	10.19	2.90	1.60	0.64	98.93	44.1
021	42.42	3.17	13.79	13.59	0.18	7.56	13.59	2.73	1.12	0.81	98.96	30.2
022	42.94	2.60	14.42	13.48	0.16	10.05	11.35	2.66	1.30	0.63	99.59	36.6
024	46.57	2.21	14.38	10.41	0.15	10.81	10.45	2.80	0.68	0.58	99.04	43.7
029	45.25	1.91	13.71	10.79	0.14	11.49	10.98	2.65	1.19	0.56	98.67	44.0
033	44.89	1.89	14.98	11.40	0.15	10.55	10.57	2.70	1.51	0.57	99.21	40.3
037	45.08	2.45	14.22	11.67	0.17	11.48	9.22	2.80	1.66	0.63	99.38	41.6
038	42.76	2.80	14.15	12.88	0.18	9.87	10.98	2.67	1.51	0.77	98.57	36.7
045	44.47	2.48	14.70	12.41	0.17	9.38	10.38	2.74	1.77	0.77	99.27	35.7
047	44.62	2.14	13.17	11.23	0.15	11.36	11.36	2.72	1.40	0.77	98.93	42.5
050	46.43	2.54	14.62	12.58	0.18	8.09	10.18	2.71	0.92	0.84	99.09	33.3

Table 5

(Con't)

Sample	SiO_2	TiO_2	Al_2O_3	FeO*	MnO	MgO	CaO	Na_2O	K_2O	P_2O_5	Total	S.I.
052	45.23	2.44	14.76	12.30	0.18	9.63	9.62	2.74	1.66	0.65	99.21	36.6
053	46.41	1.96	15.08	12.25	0.15	9.22	9.55	2.74	1.33	0.57	99.26	36.1
060	46.00	2.39	15.04	12.19	0.18	9.00	9.63	2.75	1.68	0.65	99.51	35.1
061	44.59	2.19	15.19	10.90	0.14	11.60	9.45	2.22	1.71	0.54	98.53	43.9
063	45.46	2.60	13.49	11.00	0.12	12.94	9.27	3.15	0.79	0.55	99.37	46.4
067	45.64	2.27	15.04	12.35	0.19	8.90	10.43	2.70	1.28	0.82	99.62	35.3
075	47.44	1.66	15.37	11.17	0.13	10.14	8.47	2.72	1.74	0.63	99.47	39.3
076	44.37	1.98	15.25	11.65	0.14	10.69	10.95	2.64	1.34	0.67	99.68	40.6
077	44.26	2.41	14.67	11.71	0.17	11.19	10.58	2.64	1.42	0.53	99.58	41.5
083	45.17	2.26	14.42	12.72	0.18	8.36	11.17	2.81	1.26	0.68	99.03	33.2
088	45.50	2.32	15.67	12.81	0.18	8.40	8.52	2.72	1.85	0.75	98.72	32.6
088A	46.97	2.19	14.40	12.22	0.18	9.54	8.05	3.01	2.23	0.61	99.40	35.3
095	46.08	2.22	15.23	12.05	0.19	9.83	9.20	2.75	1.58	0.71	99.84	37.5
102	45.38	2.40	14.19	13.13	0.19	8.95	9.04	2.89	1.72	0.66	98.55	33.5

Table 5

(Con't)

Sample	SiO_2	TiO_2	Al_2O_3	FeO*	MnO	MgO	CaO	Na_2O	K_2O	P_2O_5	Total	S.I.
201	46.25	2.19	14.01	11.58	0.18	10.62	9.71	2.95	0.96	0.55	99.00	40.7
205	44.07	2.30	12.92	12.09	0.20	11.54	10.31	2.88	1.41	0.63	98.35	41.3
206	44.28	2.49	13.61	11.48	0.19	12.53	9.94	3.00	1.45	0.63	99.60	44.0
208	45.15	2.61	13.21	11.18	0.19	12.25	9.82	2.97	0.76	0.67	98.81	45.1
210	44.71	2.56	14.09	12.12	0.19	10.65	9.50	2.88	1.68	0.68	99.06	39.0
211	44.55	2.56	14.55	12.74	0.19	9.51	9.23	2.82	1.81	0.71	98.67	35.4
212	43.66	2.40	13.70	11.98	0.17	11.94	9.95	2.84	1.60	0.63	98.87	35.4
213	44.13	2.50	13.82	12.42	0.19	10.61	9.45	2.83	1.69	0.65	98.29	38.5
215	44.17	2.40	13.91	11.71	0.18	12.19	9.72	2.72	1.38	0.56	98.94	43.5
216	44.20	2.24	13.24	11.11	0.18	13.23	9.67	2.87	1.46	0.60	98.80	46.2
221	44.24	2.46	13.59	11.56	0.19	12.42	9.77	2.92	1.20	0.68	99.03	44.2
222	45.96	2.38	14.22	11.64	0.17	11.07	9.59	2.88	1.13	0.54	99.58	41.43
223	45.06	2.51	14.44	12.51	0.19	9.80	9.06	2.89	1.71	0.64	98.81	36.4
226	45.63	2.01	13.20	11.09	0.17	12.25	10.75	2.75	0.61	0.50	98.96	45.8

Table 5

(Con't)

Sample	SiO_2	TiO_2	Al_2O_3	FeO*	MnO	MgO	CaO	Na_2O	K_2O	P_2O_5	Total	S.I.
231	44.87	2.43	14.10	12.20	0.19	10.76	9.17	2.96	1.74	0.70	99.12	38.9
232	45.95	2.47	14.42	12.90	0.20	8.61	8.47	2.85	1.85	0.72	98.44	32.9
233	45.90	2.42	14.26	12.75	0.20	9.11	8.48	2.98	1.87	0.72	98.69	34.1
241	43.53	2.39	13.53	12.54	0.18	10.50	10.71	2.85	1.63	0.65	98.51	38.2
Average	44.97	2.36	14.28	11.96	0.17	10.43	9.97	2.79	1.42	0.65	99.00	39.0
S.D.	1.11	0.25	0.67	0.74	0.01	1.42	1.01	0.14	0.35	0.08		

MgO range = 7.56 to 13.23

* Total Fe as FeO

S.I. = $100MgO/(MgO + FeO + K_2O + Na_2O)$

Table 6

Analysis of Basaltic Andesite, Volcanic Bombs, and Basalt Dike

Sample	SiO_2	TiO_2	Al_2O_3	FeO*	MnO	MgO	CaO	Na_2O	K_2O	P_2O_5	Total	S.I.
Basaltic Andesite												
209	52.32	2.19	14.71	12.63	0.19	4.70	7.75	3.02	1.39	0.41	99.31	21.7
242	53.82	2.16	14.24	10.86	0.14	5.90	6.88	3.19	1.52	0.47	99.18	27.5
Volcanic Bombs												
227	45.46	1.94	13.41	11.34	0.19	12.25	10.71	2.78	1.23	0.61	99.92	____
296	45.77	2.28	13.88	11.97	0.19	10.00	10.36	2.87	1.53	0.71	99.83	____
Basalt Dike												
067	45.19	2.46	15.09	12.22	0.15	7.66	11.85	3.11	1.18	0.70	99.61	____

* Total Fe as FeO

S.I. = 100 MgO/(MgO + FeO + K_2O + Na_2O)

A	andesites
B	basalts
Ba	basanites
BaA	basaltic andesites
Be	benmoreites
D	dacites
H	hawaiites
M	mugearites
Ne	nephelinites
P	phonolites
PN	phonolitic nephelinites
PrB	picrite basalts
PT	phonolitic tephrites
R	rhyolites
Te	tephrites
Tr	trachytes
Tra	trachyandesites
Trb	trachybasalts

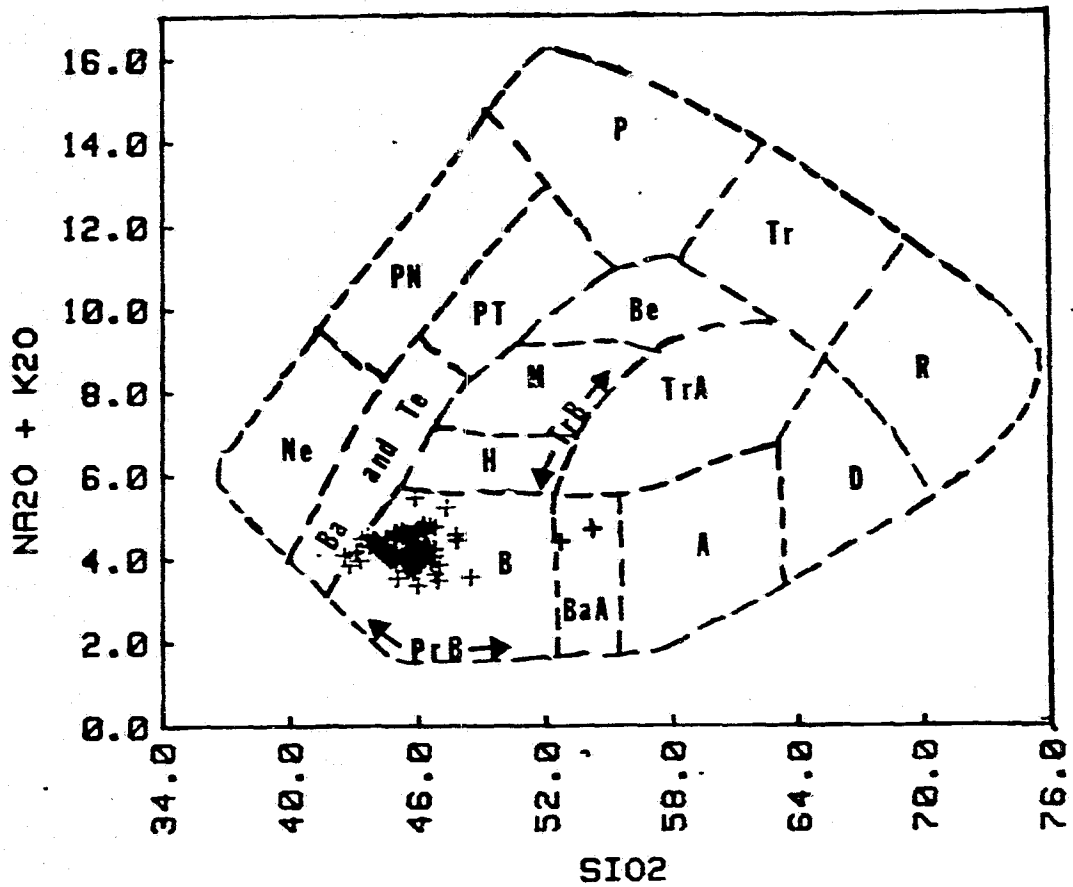

Figure 3 Plot of alkali versus silica for West Potrillo Basalt samples; classification after Cox et al. (1979).

The basalt flow samples were then divided into alkaline and subalkaline. This is shown in Figure 4 using a plot of Ne-Q-Ol normative compositions. The two samples that plot as subalkaline correspond to the samples that are shown to be basaltic andesite in composition in Figure 3. It should be noted that seven samples plot in between Poldervaart's (1964) divider and Irvine and Barager's (1971) divider. These samples contain small amounts of normative hypersthene and can be plotted as subalkaline. For the purposes of chemical classification, these samples will be classsified subalkaline based on the Irvine and Barager (1971) divider. The alkaline samples were then plotted on an Ab'-Or-An diagram (Fig. 5) and were shown to be predominantly potassic in nature. Figure 6 shows a plot of normative plagioclase composition vs normative color index identifying the alkaline samples as predominantly alkali basalts bordering ankaramite in composition. The subalkaline samples were plotted on an Al_2O_3 vs normative composition diagram (Fig. 7) and were shown to be high magnesium tholeiitic basalts. The phenocontemporaneous eruption of both tholeiitic and alkali basalts is similar to volcanism reported in other areas of the Rio Grande Rift (Baldridge, 1979).

The trend of the basalt flows toward an increase in iron with a corresponding decrease in magnesium is shown in Figure 8. The normative mineralogy of the volcanic rocks of the West Potrillo is shown in Figure 9 and shows a trend from low hypersthene to an increase in normative nepheline.

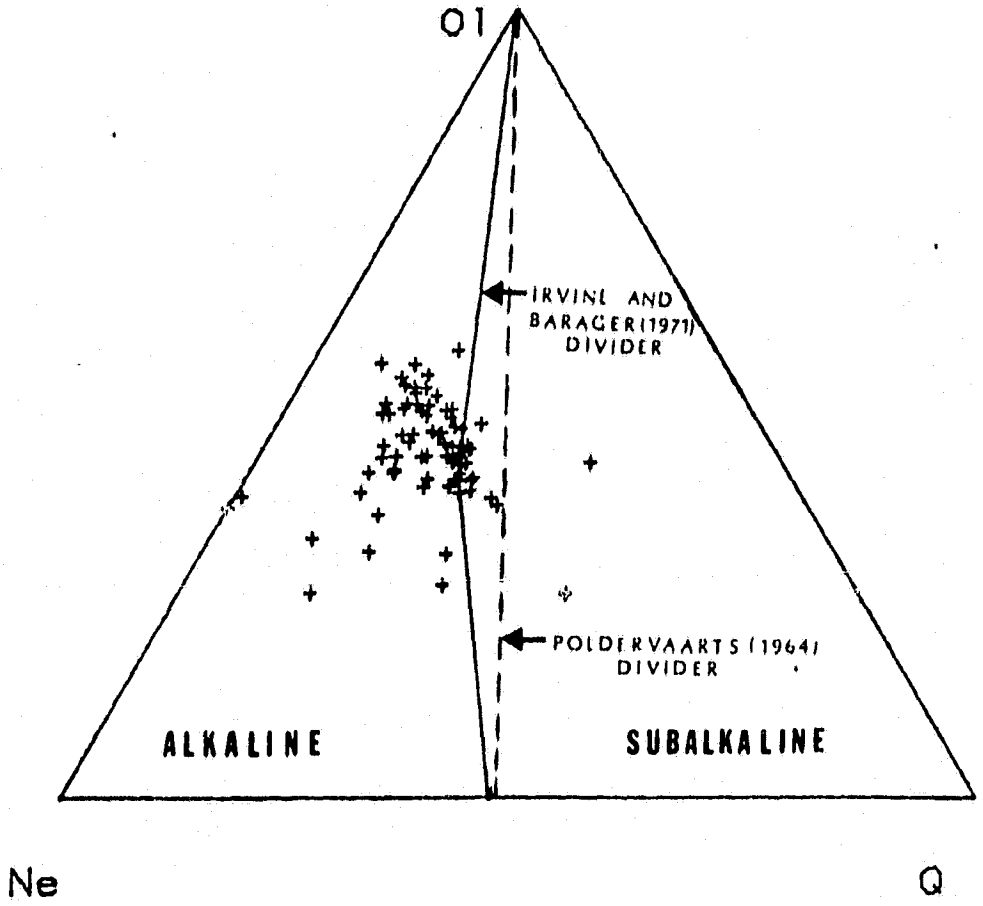

Figure 4 Ne-Q-Ol projection, alkaline versus subalkaline plot. Note Poldevaarts(1964) dividing plane for separating tholeiitic and alkaline rocks. Also Irvine and Baragers(1971) proposed dividing plane. Plots in percent cation equivalents. (after Irvine and Barager, 1971)

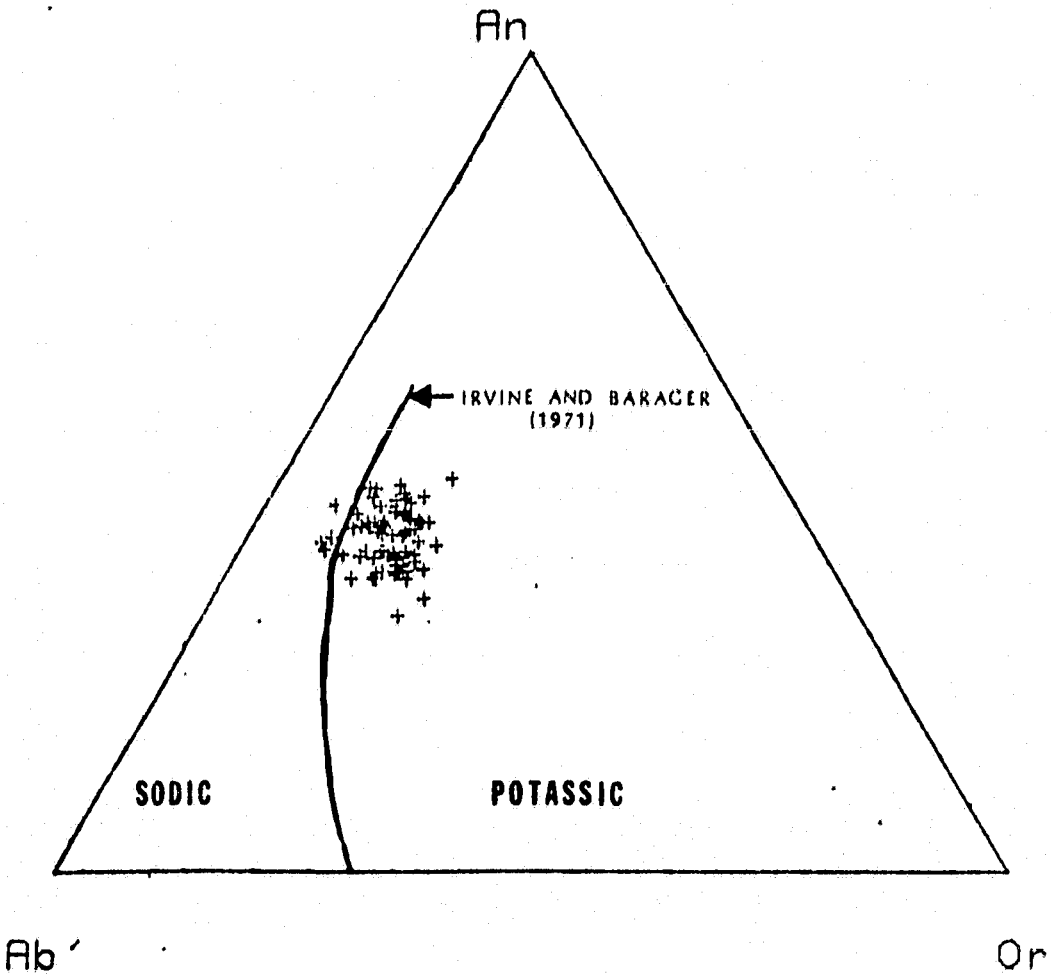

Figure 5 Ab'-Or-An projection, sodic versus potassic series. Note Irvine and Baragers(1971) dividing line between the sodic and potassic series. Plots in percent cation equivalents. (after Irvine and Barager, 1971)

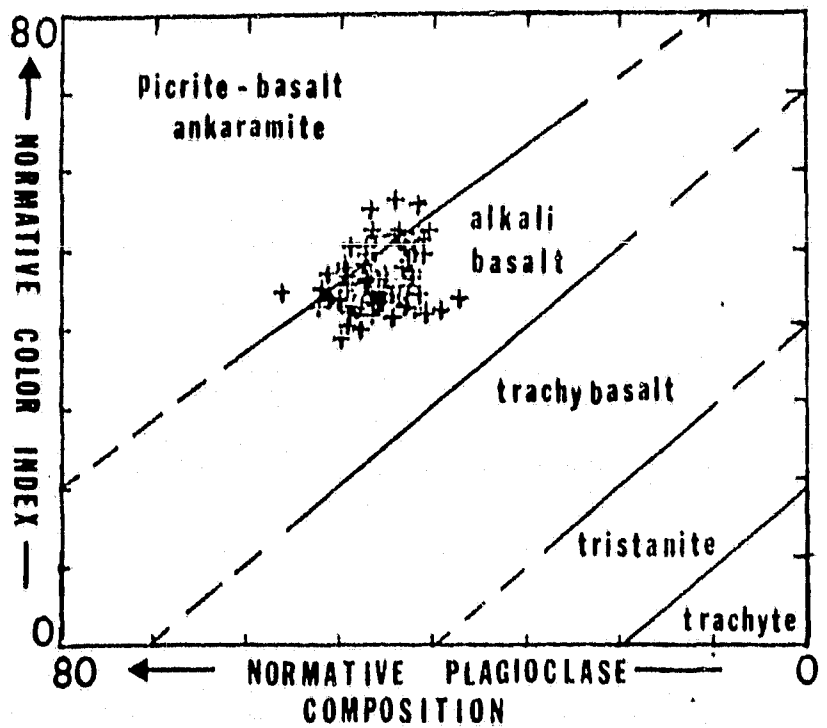

Figure 6 Plot of Normative Color Index versus Normative Plagioclase Composition. Plots in percent cation equivalents. (after Irvine and Barager, 1971)

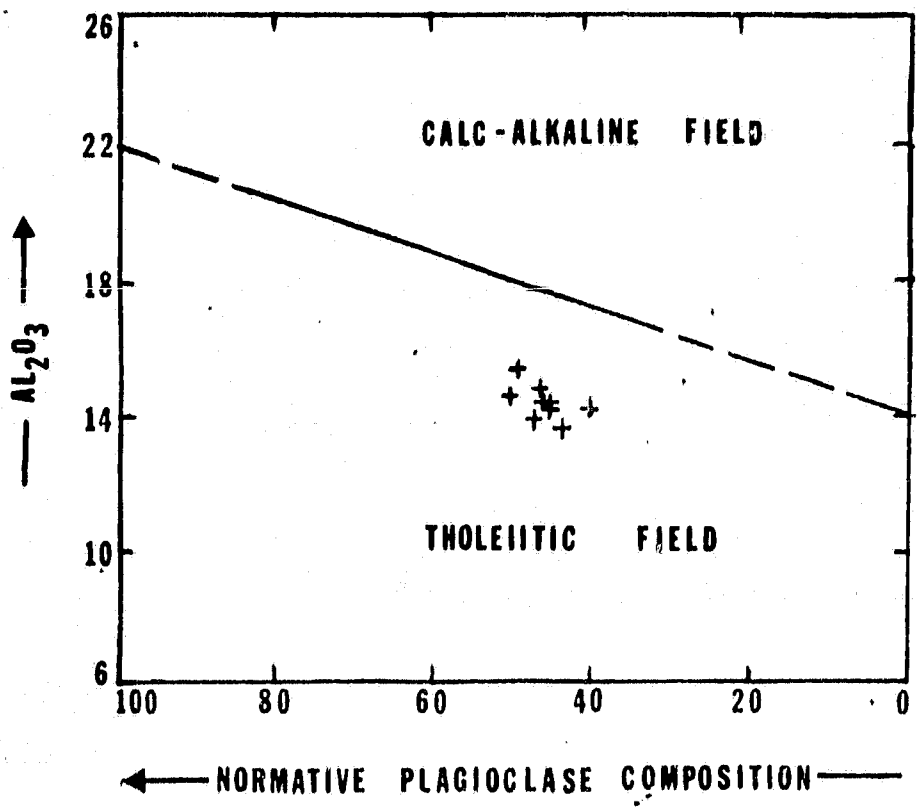

Figure 7 Plot in wt. percent Al_2O_3 versus normative Plagioclase Composition. Note the dividing line of Irvine and Barager(1971) for calc-alkaline and tholeiitic fields. (after Irvine and Barager, 1971)

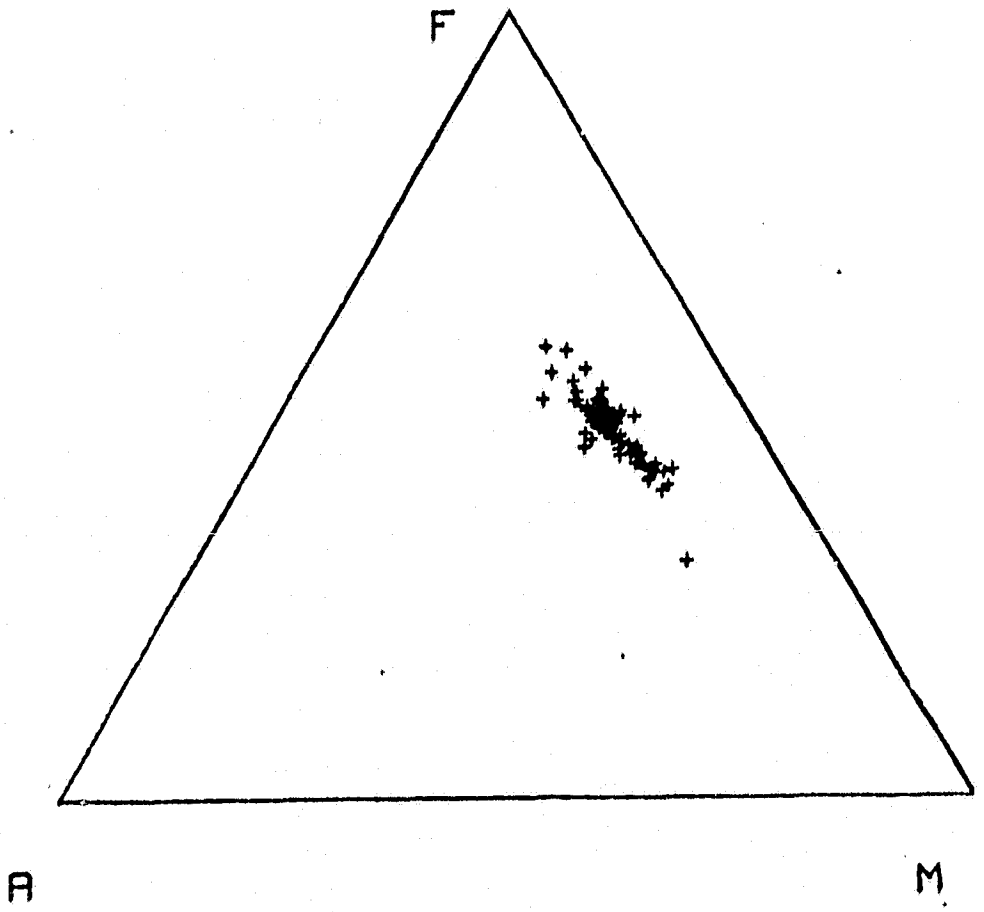

Figure 8 A-F-M projection, plot in weight percent.

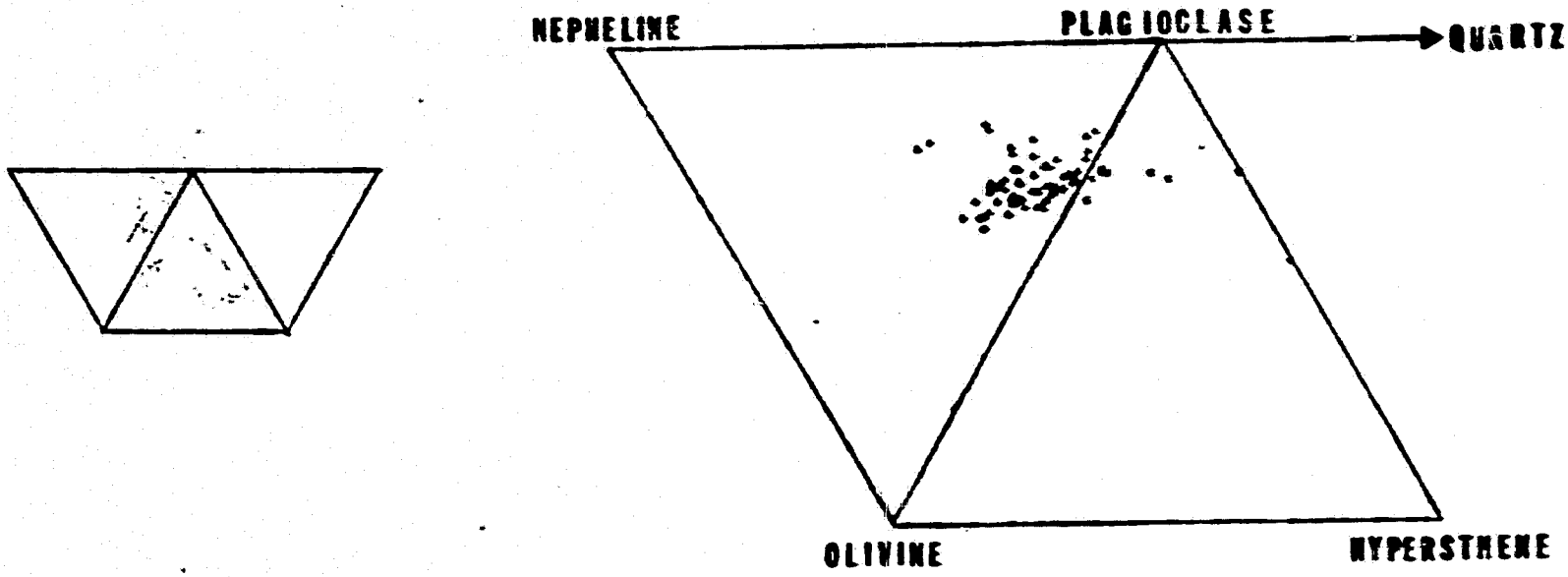

Figure 9 Plot of normative mineralogy of West Potrillo Basalt field, New Mexico. (after Baldridge, 1979)

Chemical Variations

The alkali-olivine basalts of the West Potrillo Basalt field were divided into two members based on petrography by Hoffer (1976). The author completed 75 new chemical analysis of the West Potrillo basalts and divided them into Members 1 and 2 based on the petrography described by Hoffer (1972) and Bersch (1977). The results of these analysis are reported in Tables 4 and 5. The analysis show an average MgO content in Member 1 of 8.67% with Member 2 showing an average MgO content of 10.43%. This supports Hoffer (1976) in his statement that Member 2 has a higher MgO content than Member 1. It should be noted, however, that a considerable overlap does exist in MgO contents, between the two members.

Member 1 has an average solidification index of 34, and Member 2 has an average solidification index of 39. The solidification index decreases with decrease in proportion of liquid remaining from differentiation. Values of SI less than 35 are thought to result from within crust differentiation of basaltic magma, 35 to 40 imply little or no differentiation, and values greater than 40 suggest accumulation of olivine crystals (Kuno, 1968; Renault, 1970). This suggests that Member 1 and 2 are only slightly differentiated.

Mineralogical vs Chemical Variations

A discriminant analysis was completed on the alkali-olivine basalt members to determine if any relationship exists between the petrological divisions and the chemical analyses of

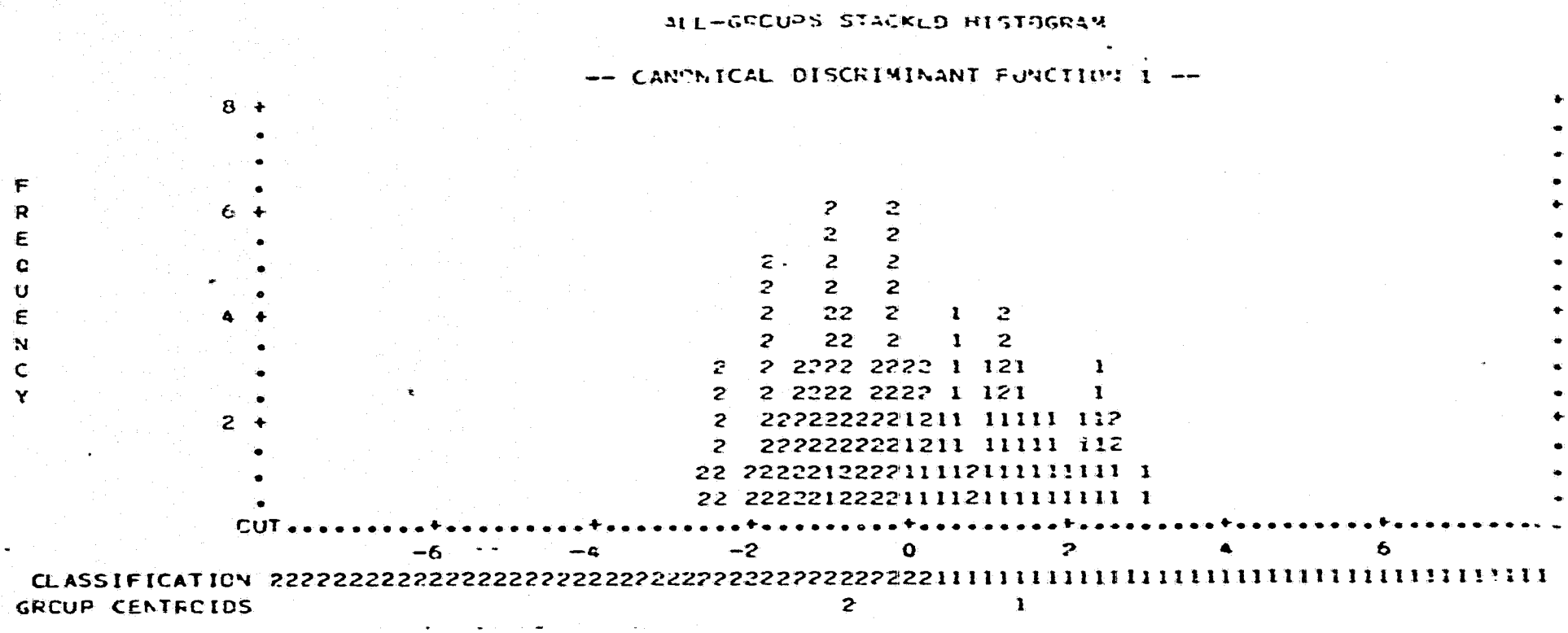

CLASSIFICATION RESULTS -

ACTUAL GROUP	NO. OF CASES	PREDICTED GROUP MEMBERSHIP 1	2
GROUP 1	30	26	4
SUBFILE M1		86.7%	13.3%
GROUP 2	45	4	41
SUBFILE M2		8.9%	91.1%

PERCENT OF "GROUPED" CASES CORRECTLY CLASSIFIED: 89.33

Figure 10 Discriminant plot Member 1 vs Member 2.

the members (Tables 4 and 5). The analysis showed that MgO, CaO and TiO_2 concentrations are the most powerful discriminating variables between the members. The results of this analysis are shown in Figure 10. The division of samples into Members 1 and 2 based on the petrography can be supported by the geochemical variations up to 89.3% accuracy of classification.

Volcanic Bombs and Dike

Two analysis of volcanic bombs and one dike were completed (Table 6). Both the volcanic bombs show high concentrations of MgO and the basalt dike a lower concentration.

Feldspar Megacrysts

Introduction

Fifty feldspar megacrysts were chemically analyzed by x-ray fluorescence (Table 7). The samples were selected for their size, exceeding 3 mm in length, and their lack of any remnant pieces of basalt matrix or excessive weathering (Appendix D). The feldspar megacrysts were classified according to the classification of Muir (1961).

Classification

Normative Or, Ab and An were calculated for the 50 feldspar megacrysts and plotted on a standard Or-Ab-An triangle (Fig. 11). The megacrysts consist of andesine, oligoclase, potash oligoclase, limestone anorthoclase, and anorthoclase. The majority of the megacrysts fall into the anorthoclase and

Table 7 Analysis of Feldspar Megacrysts

	An-orthoclase	An-orthoclase	Oligoclase	Lime An-orthoclase	An-orthoclase	Andesine	An-orthoclase	Potash Oligoclase	An-orthoclase	Potash Oligoclase
Sample	13-A	13-C	13-L	33-A	54-M	551-A	56-K	57-A	57-K	61-K
SiO_2	64.67	64.21	60.20	64.86	64.24	59.62	64.84	61.50	64.25	63.68
TiO_2	0.01	0.01	0.03	0.00	0.01	0.03	0.02	0.02	0.01	0.03
Al_2O_3	21.26	21.22	24.88	21.27	21.41	25.59	21.36	24.19	21.40	22.43
Fe_2O_3	0.29	0.37	0.11	0.23	0.57	0.11	0.14	0.15	0.37	0.30
MnO	0.00	0.00	0.00	0.00	0.00	0.00	0.00	0.00	0.00	0.00
MgO	0.01	0.00	0.12	0.02	0.00	0.21	0.02	0.11	0.00	0.03
CaO	1.84	2.04	5.07	1.86	1.76	6.04	1.47	4.91	1.73	2.86
Na_2O	7.59	7.91	7.90	6.56	8.26	6.97	8.73	7.45	8.80	7.63
K_2O	3.59	3.26	1.10	3.72	2.92	1.16	3.15	1.52	2.55	1.90
Total	99.26	99.02	99.41	98.52	99.17	99.73	99.73	99.85	99.11	98.86
*Ab%	69.15	70.69	69.10	65.32	74.01	62.91	75.12	66.70	76.93	72.90
*Or%	21.57	19.22	6.35	24.43	17.26	6.91	17.88	8.97	14.70	11.97
*An%	9.28	10.09	24.55	10.25	8.73	30.18	7.00	24.33	8.37	15.13
Total	100.0	100.0	100.0	100.0	100.0	100.0	100.0	100.0	100.0	100.0

* Recalculated on the basis of 100%.

Table 7 - (Con't)

	An-orthoclase	Potash Oligoclase	Lime An-orthoclase	Potash Oligoclase	An-orthoclase	An-orthoclase	Oligoclase	Andesine	An-orthoclase	Lime An-orthoclase
Sample	62-A	621-I	621-J	621-L	63-K	63-S	63-T	64-M	64-N	64-Q
SiO_2	63.91	63.00	64.10	63.30	64.49	63.27	60.12	60.48	64.64	62.64
TiO_2	0.00	0.01	0.00	0.02	0.00	0.01	0.02	0.02	0.02	0.00
Al_2O_3	22.01	22.31	21.79	22.62	21.69	21.59	24.33	24.72	21.17	21.93
Fe_2O_3	0.25	0.47	1.05	0.15	0.06	1.15	0.09	0.47	0.23	3.09
MnO	0.00	0.00	0.00	0.00	0.00	0.00	0.00	0.00	0.00	0.00
MgO	0.03	0.01	0.00	0.05	0.06	0.00	0.06	0.08	0.00	0.01
CaO	1.86	2.85	2.14	2.63	1.88	2.00	4.43	5.43	1.56	1.90
Na_2O	8.36	8.58	7.69	7.92	7.29	9.55	9.63	7.01	9.26	8.16
K_2O	2.89	1.72	2.93	1.93	3.21	2.21	1.09	1.16	2.99	1.81
Total	99.31	98.95	99.70	98.61	98.68	99.78	99.77	99.37	99.87	99.54
*Ab%	74.01	75.98	71.16	74.37	71.49	78.83	75.23	65.02	76.56	78.42
*Or%	16.88	10.05	17.88	11.95	19.11	12.03	5.62	7.10	16.30	11.47
*An%	9.12	13.97	10.96	13.67	9.39	9.14	19.16	27.88	7.14	10.11
Total	100.0	100.0	100.0	100.0	100.0	100.0	100.0	100.0	100.0	100.0

Table 7 (Con't)

	An-orthoclase	Lime An-orthoclase	An-orthoclase	Oligoclase	Oligoclase	Oligoclase	An-orthoclase	Lime An-orthoclase	Potash Oligoclase	An-orthoclase
Sample	660	66-X	66-Y	67-C	68-F	75-F	75-M	751-E	751-P	76-B
SiO_2	64.23	63.06	64.76	60.05	61.11	61.21	65.06	63.45	63.04	64.48
TiO_2	0.00	0.02	0.00	0.03	0.02	0.03	0.02	0.00	0.02	0.01
Al_2O_3	21.40	22.64	21.56	25.16	24.44	23.43	21.19	22.33	22.84	21.65
Fe_2O_3	0.74	0.05	0.05	0.18	0.47	2.09	0.05	0.83	0.09	0.25
MnO	0.00	0.00	0.00	0.00	0.00	0.00	0.00	0.00	0.00	0.00
MgO	0.00	0.10	0.08	0.14	0.08	0.00	0.05	0.02	0.06	0.02
CaO	1.94	2.85	1.60	5.32	4.86	4.72	1.67	2.23	2.84	1.70
Na_2O	8.32	7.61	8.58	7.72	7.68	6.75	7.05	8.02	7.93	8.47
K_2O	2.64	2.39	3.25	1.19	1.26	1.13	3.35	2.86	1.67	2.80
Total	99.27	98.72	99.88	99.79	99.92	99.36	98.44	99.74	98.49	99.38
*Ab%	74.72	70.70	73.91	67.42	68.56	66.78	69.23	71.99	74.79	75.24
*Or%	15.64	14.64	18.46	6.86	7.42	7.37	21.70	16.93	10.39	16.40
*An%	9.64	14.66	7.63	25.72	24.02	25.85	9.08	11.08	14.83	8.36
Total	100.0	100.0	100.0	100.0	100.0	100.0	100.0	100.0	100.0	100.0

Table 7 (Con't)

	Potash Oligoclase	Oligoclase	Potash Oligoclase	Lime An-orthoclase	Lime An-orthoclase	Oligoclase	Lime An-orthoclase	Lime An-orthoclase	Lime An-orthoclase	Potash Oligoclase
Sample	204-A	215-B	215-C	215-D	216-A	217-A	217-L	217-M	218-M	218-N
SiO_2	62.04	60.76	61.06	62.29	64.51	60.15	64.06	64.13	63.97	61.78
TiO_2	0.02	0.03	0.02	0.01	0.00	0.02	0.02	0.00	0.01	0.02
Al_2O_3	23.65	24.16	24.90	22.80	21.94	24.60	21.88	22.26	22.06	24.06
Fe_2O_3	0.05	0.19	0.05	0.22	0.07	0.24	0.24	0.21	0.18	0.20
MnO	0.00	0.00	0.00	0.00	0.00	0.00	0.00	0.00	0.00	0.00
MgO	0.19	0.18	0.38	0.15	0.07	0.29	0.07	0.17	0.03	0.14
CaO	3.78	3.89	5.02	2.70	2.10	4.22	2.22	2.55	2.39	4.90
Na_2O	8.31	8.22	6.37	8.43	6.96	8.57	7.16	6.00	7.06	6.80
K_2O	1.54	1.31	1.58	2.83	3.25	1.38	3.06	3.72	2.83	1.39
Total	99.58	98.74	99.38	99.43	98.90	99.47	98.71	99.04	98.53	99.29
*Ab%	72.78	73.15	62.51	71.49	67.80	72.53	68.80	60.82	68.88	65.20
*Or%	8.90	7.69	10.23	15.83	20.88	7.70	19.39	24.87	18.21	8.79
*An%	18.33	19.16	27.27	12.68	11.32	19.77	11.81	14.31	12.91	26.01
Total	100.0	100.0	100.0	100.0	100.0	100.0	100.0	100.0	100.0	100.0

Table 7 (Con't)

	An-orthoclase	An-orthoclase	Oligoclase	Potash Oligoclase	Potash Oligoclase	An-orthoclase	An-orthoclase	An-orthoclase	An-orthoclase	Oligoclase
Sample	272-A	272-C	272-E	272-K	272-L	274-A	274-F	274-G	276-A	282-B
SiO_2	64.35	65.21	60.79	63.09	62.74	65.12	65.25	64.80	64.56	58.50
TiO_2	0.00	0.01	0.03	0.01	0.01	0.02	0.00	0.01	0.01	0.02
Al_2O_3	21.07	20.53	24.33	23.03	23.73	20.64	21.08	21.33	21.11	25.99
Fe_2O_3	0.15	0.14	0.20	0.22	0.33	0.13	0.05	0.10	0.17	0.24
MnO	0.00	0.00	0.00	0.00	0.00	0.00	0.00	0.00	0.00	0.00
MgO	0.05	0.03	0.14	0.11	0.40	0.03	0.07	0.03	0.07	0.44
CaO	1.22	0.94	4.90	3.63	4.59	1.06	1.09	1.91	1.24	5.67
Na_2O	7.83	8.01	7.91	7.04	6.12	7.38	7.21	8.16	8.64	7.66
K_2O	4.54	4.99	1.10	1.88	2.05	4.68	4.21	2.95	4.13	1.19
Total	99.21	99.86	99.40	99.01	99.97	99.06	98.96	99.29	99.93	99.71
*Ab%	68.09	67.76	69.70	68.42	61.12	66.77	68.08	73.10	71.70	66.13
*Or%	26.04	27.84	6.39	12.05	13.50	27.93	26.22	17.43	22.61	6.78
*An%	5.87	4.40	23.90	19.53	25.38	5.31	5.70	9.47	5.70	27.10
Total	100.0	100.0	100.0	100.0	100.0	100.0	100.0	100.0	100.0	100.0

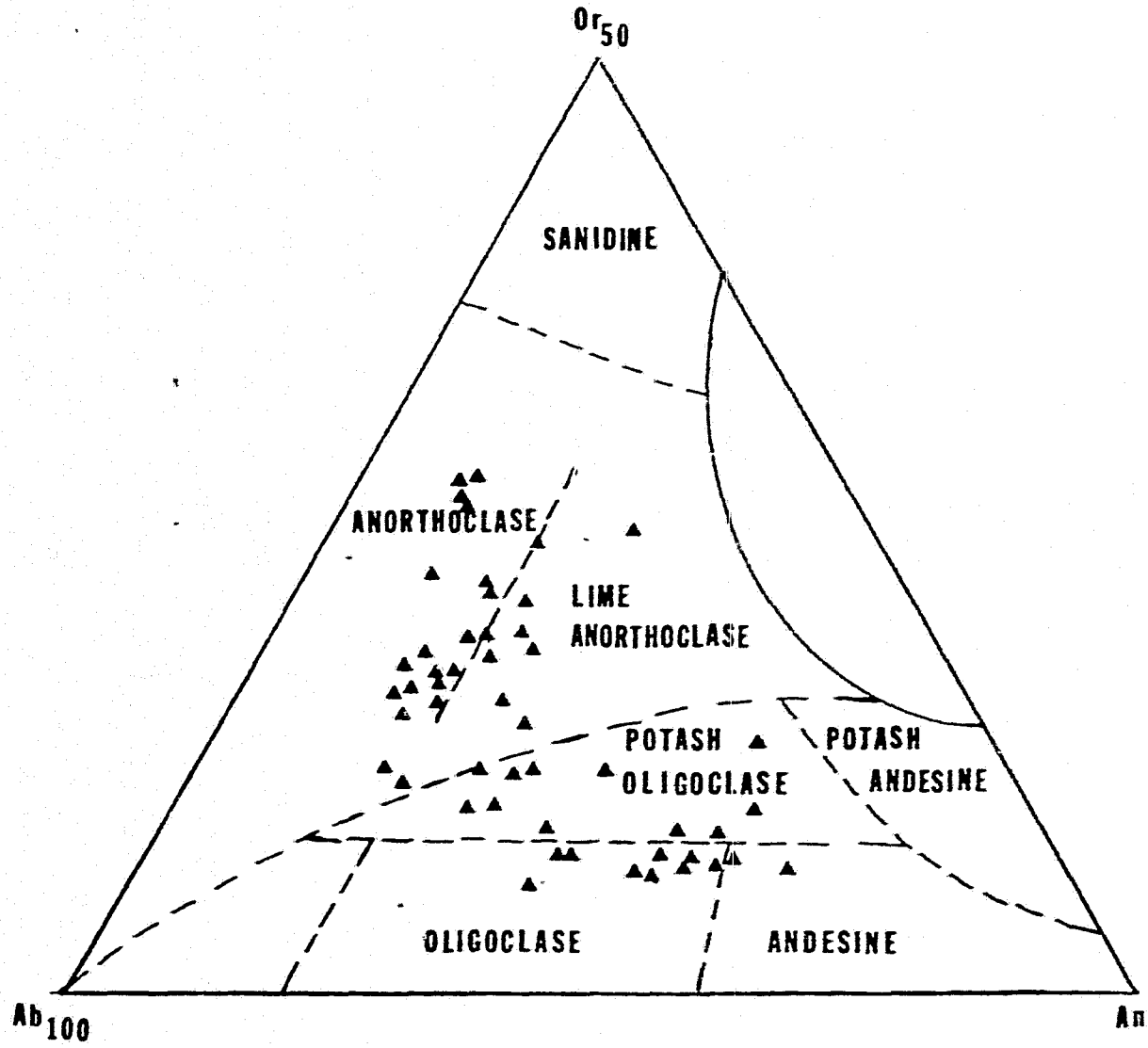

Figure 11 Molecular composition of feldspar megacrysts in West Potrillo Basalt, New Mexico. Recalculated to Or,Ab and An content. Based on classification of Muir(1961) where Or is $KAlSi_3O_8$, Ab is $NaAlSi_3O_8$ and An is $CaAlSi_2O_8$.

oligoclase fields with a trend extending from andesine, oligoclase to potash oligoclase. No relationship could be determined between location and composition of feldspar megacrysts.

Interpretation

The high alkali content of the basalt can account for the presence of both anorthoclase and K-oligoclase.

Ortiz (1979) states that the normative feldspar compositions of the host basalt plot within the excluded portion of the Or-Ab-An diagram. This indicates that alkali-rich and calcic plagioclases could have crystallized from the melt and co-existed in equilibrium at high temperature and pressure (Laughlin and others, 1974).

COMPARISON TO AREA BASALT FLOWS

Basalt flows in the immediate area include the Black Mountain-Santo Tomas, Aden, Afton flows. The Black Mountain-Santa Tomas basalts are alkali-olivine basalts. They are porphyritic and hypocrystalline with phenocrysts ranging in size from 0.5 to 2 mm. Eudhedral to subhedral crystals of plagioclase feldspar, olivine, and phyroxene, comprise 15 to 30% of the rock. The groundmass consists of plagioclase laths 0.1 mm in length and small anhedral grains of pyroxene, magnetite, and light- to dark-colored interstitial glass. Glomeroporphyritic accumulations of olivine are also common (Hoffer, 1969). The Afton Basalt are alkali-olivine basalts, hypocrystalline, microporphyritic, and vesicular. Microphenocrysts average 15% and are composed of olivine and minor plagioclase. The Aden Basalt are hypocrystalline and microporphyritic with subhedral to euhedral microphenocrysts of plagioclase, olivine and pyroxene set in a fine-grained groundmass of subhedral plagioclase, pyroxene and glass. Microphenocrysts average less than 15%, and are less than 1 mm in diameter and commonly glomeroporphyritic (Hoffer, 1976). The Black Mountain-Santo Tomas, Aden, Afton basalts contain higher concentrations of modal olivine than the West Potrillo Basalts.

The average chemical compositions of the West Potrillo basalts are plotted in Figure 12 on an AFM diagram, where MgO = SI. The solidification Index, SI, of Kuno et al. (1957) indi-

cates the extent of differentiation (Renault, 1970).

Based on the Solidification Index the two tholeiitic samples (209, 242) and the average Member 1 from the West Potrillo field plot on the AFM diagram with an SI less than 35 indicating differentiation of the basaltic magma within the crust. The average Member 2 of the West Potrillo field plots between an SI of 35 and 40 indicating little or no differentiation from primary basalt magma, and the flows of the Aden-Afton and Black Mountain-Santo Tomas plot above an SI of 40 indicating accumulations of olivine crystals.

The lack of differentiation implies that basaltic magma was probably derived directly from the mantle (Renault, 1970). Differences in the SI of the West Potrillo basalt Member 1 and 2 could be due to the tapping from different levels of a differentiated magma chamber. The Rio Grande rift is a possible mechanism for transport of the magma from the mantle.

AD ADEN
AF AFTON
B BLACK MOUNTAIN
WEST POTRILLO
P1 MEMBER ONE
P2 MEMBER TWO
209 THOLEIITIC
242
S SANTO TOMAS

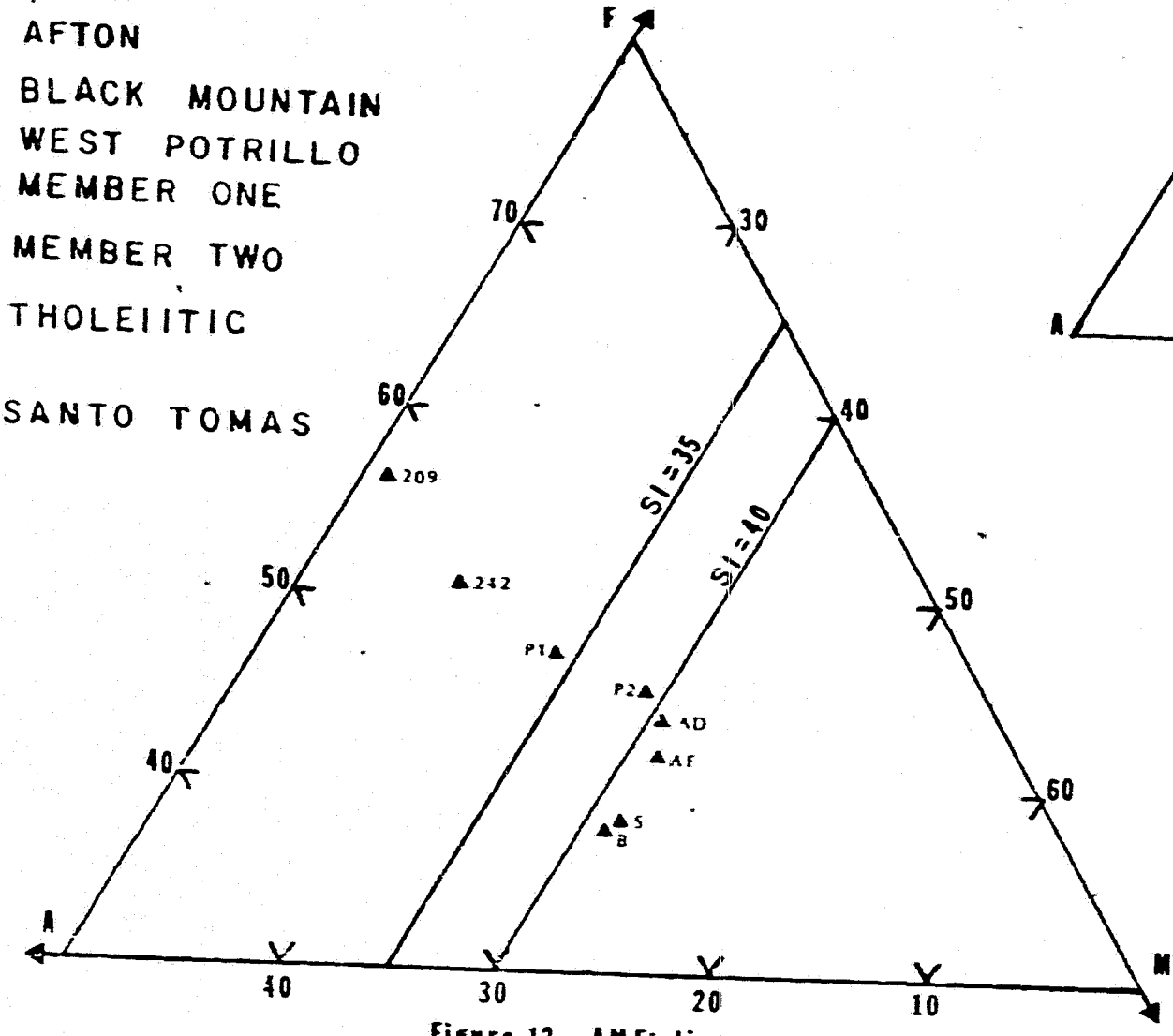

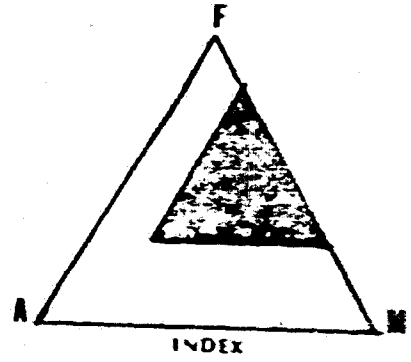

Figure 12 AMF diagram
AFTER RENAULT (1970)

DISCUSSION

The alkali olivine basalts of the West Potrillo Basalt field are classified as within Plate Basalts based on the classificition of Pearce (1976). This classification cannot distinguish between ocean island and continental basalts on any of the classification functions. This may mean that the generation of magmas within plate may be independent of the nature of the crust (Pearce, 1976). In relating these lavas to experimental studies it should be noted that the lava is considered to be representative of a primary (primative) magma. A primary magma is one that has been generated by partial melting of the upper mantle and was in equilibrium with a perioditic residuum at depths of 10 to 80 km in the mantle. The magma must also have been erupted to the earth's surface with little or no modification (Ringwood, 1975). Four characteristics indicate that this lava could represent a primary magma:

1) The major element criterian of primitive composition is the Mg ratio (Ringwood, 1975; Baldridge, 1979):

   $$\text{Mg ratio} = 100\,(MgO/(MgO + Fe^{++})) = 68\text{-}72$$

   Three chemical analyses were taken from Hoffer (1976). The values for FeO and Fe_2O_3 gave an average Mg ratio of 67.8 and ranged from 63.8 to 71.4 (Table 8).

2) Due to the presence of mantle xenoliths and high pressure xenocrysts (Ortiz, 1979), the eruption from the source region must have been of relatively high vel-

Table 8

	Wp-1*	Wp-2*	Wp-3*
SiO_2	44.63	44.37	44.21
TiO_2	2.60	2.37	2.21
Al_2O_3	15.92	15.98	15.01
Fe_2O_3	3.66	4.13	4.82
FeO	6.56	6.82	6.07
MnO	0.14	0.16	0.14
MgO	9.17	7.30	10.34
CaO	10.36	10.09	10.94
Na_2O	4.70	4.48	3.67
K_2O	0.90	2.27	1.65
H_2O	1.60	1.90	nd
P_2O_5	0.64	0.74	0.48
Total	100.88	100.61	99.54
Mg ratio	71.40	63.80	68.20

* — analysis from Hoffer(1976)

nd— none detected

Mg ratio = 100 * MgO/MgO + Fe^{2+}

ocity which would allow little or no fractionation during the move to the surface. Also, little or no reaction of the xenoliths with the host magma suggests rapid transport to the surface.

3) Plagioclase megacrysts from the West Potrillo basalt showed no zoning and using the Nash (1973) formula

$$P(\text{kilobars}) = -0.39(\%An) + 34.7$$

were determined by Ortiz (1977) to have formed at pressures between 18.36 kilobars to 28.01 kilobars at approximately 75 km depth.

4) Binns and others (1970) cite experimental studies indicating the tendence of plagioclase near the liquidous composition to become more sodic at high pressure. Warren and others (1979) suggested anorthoclase megacrysts in the Eagle Basin was less than 29 km. The trend toward an increase in Na and the formation of anorthoclase fit the trend of the feldspar megacrysts shown in Figure 11.

The composition of the West Potrillo Basalt field ranges from alkali-olivine basalt to olivine basanite (greater than 5% normative Ne). It is possible to obtain this trend by the fractionation of an olivine tholeiite at 13-18 kb pressure or at 27 kb pressure with a magma with 7% water. This fractionation trend is shown in Figure 13. At 13-18 kb pressure, corresponding to a depth of 35-65 km, the olivine field is largely sup-

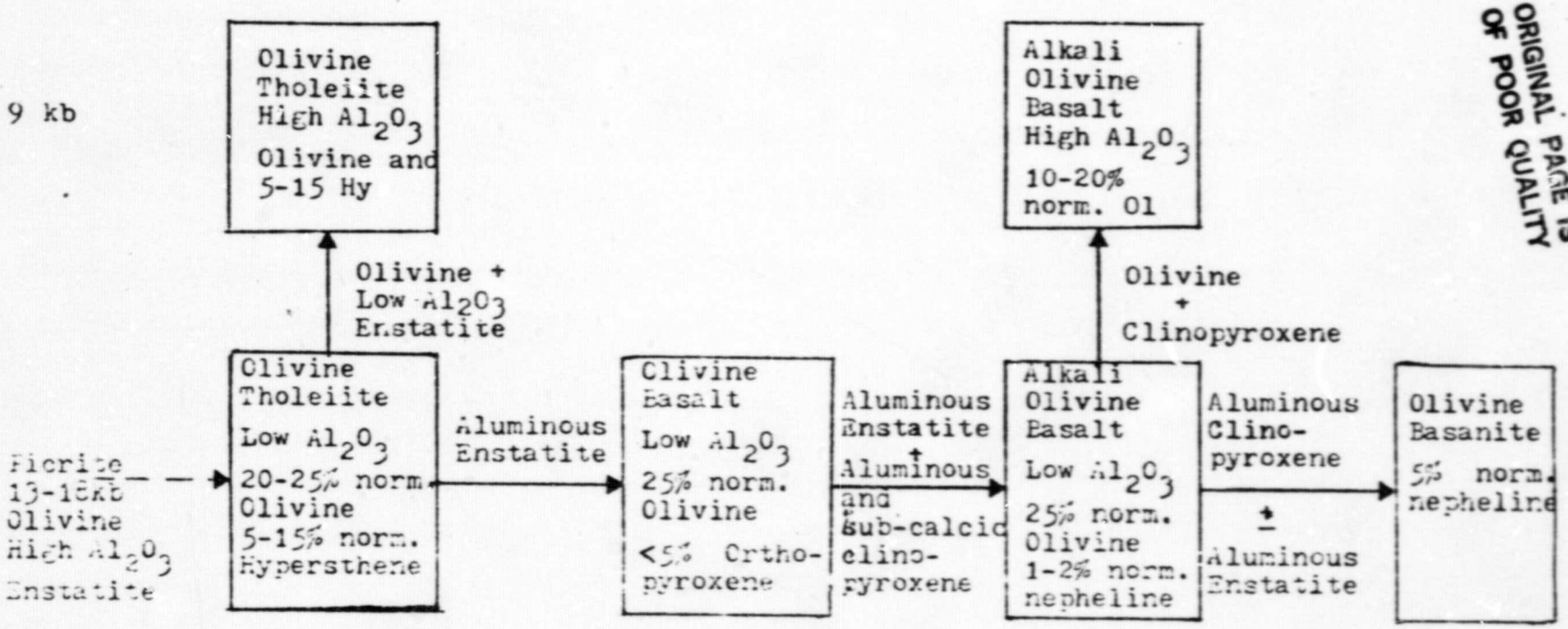

Figure 13 Fractionation diagram (after Green and Ringwood, 1967)

pressed, and crystallization is dominated by the separation of aluminous orthopyroxene ± subcalcic aluminous clinopyroxene. The residual liquids fractionate directly towards the critical plane of undersaturation and across into the alkali basalt field, yielding alkali olivine and basanites with 5% normative nepheline (Ringwood, 1975). If water (5-7%) is available in the source regions of basaltic magmas, the primary field of crystallization of orthopyroxene from alkaline basaltic magmas at high pressure is greatly extended (Bultitude and Green, 1968). Since high water contents in highly alkaline magmas frequently display explosive eruptions, the addition of the water is plausible. The addition of water allows the fractionation to occur under as much 27 kb pressure (Ringwood, 1975).

The fractionaly crystallization by separationof major orthopyroxene depletes the residual liquid in SiO_2 and enriches it in CaO and alkalis. This chemical variation is similar to known trends that are observed in mantle-derived basalts ranging in composition from alkali-olivine basalt to olivine nephelinite (Ringwood, 1975).

The West Potrillo Basalts are associated with the Rio Grande Rift. Evidence at the present time, both geological and geophysical, supports mantle upwelling under the rift. With mantle diapirism providing the mode of transport for the magma to the lower crust resulting in the eruption of the alkali-olivine basalt (Wilshire and Pike, 1975).

A hypothetical cross-section of the crust and upper mantle that could have provided the environment resulting in the transport of the magma to the surface is shown in Figure 14.

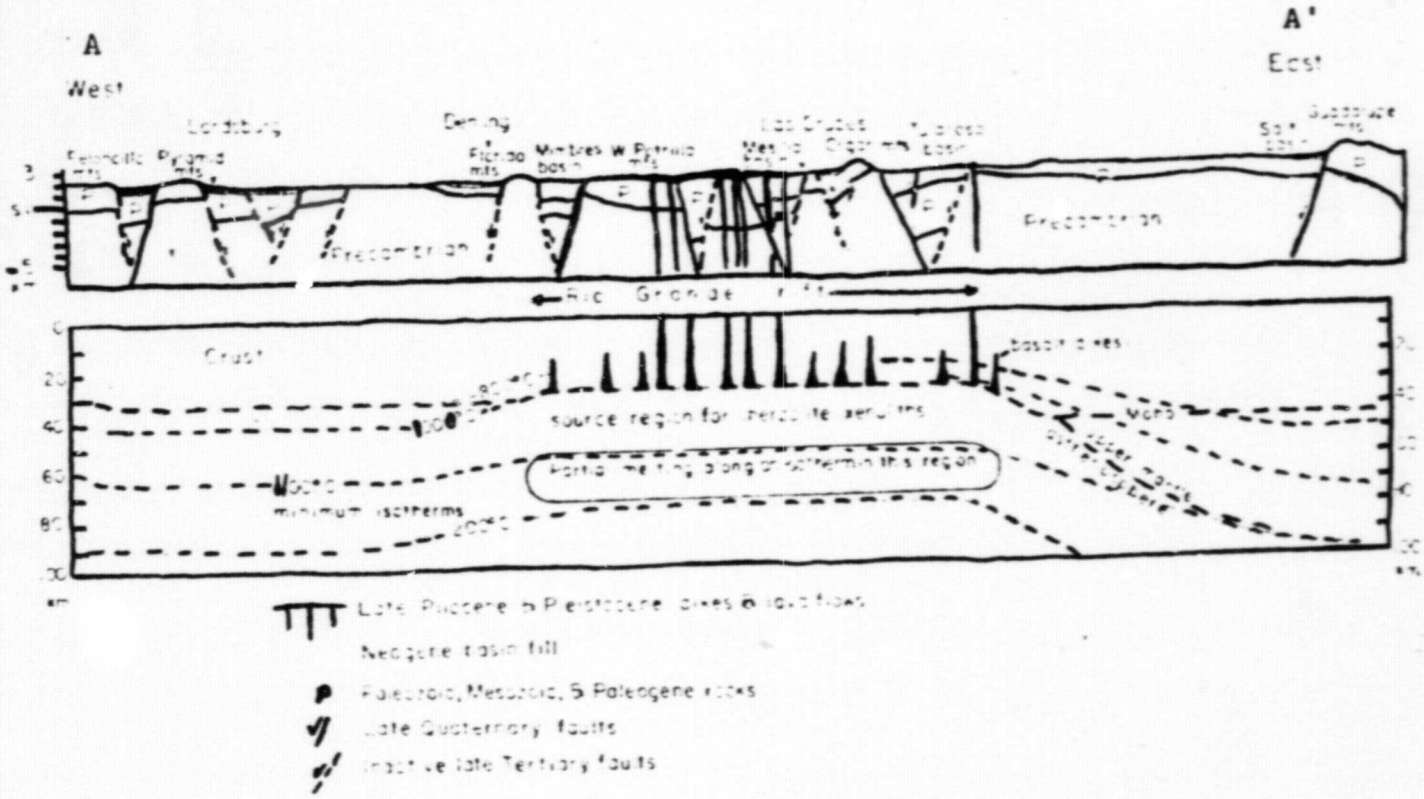

Figure 14 Interpretive cross-section A-A' (Fig. 2) of the crust and upper mantle across the southern Rio Grande rift along latitude 32°22"N (after Seager and Morgan, 1979).

CONCLUSIONS AND SUMMARY

The West Potrillo Basalt flows are hypocrystalline, microporphyritic to porphyritic with a microcrystalline groundmass. Essential minerals that occur are plagioclase, feldspar, clinopyroxene, and olivine. Accessory minerals include magnetite, illmenite, analcime, chrome spinel, serpentine, chlorite, and calcite. Feldspar occurs both in the groundmass as subhedral plagioclase laths and as alkali and plagioclase feldspar megacrysts. Based on chemistry and petrography, the West Potrillo Basalt flows have been found to consist of abundant alkali-olivine and minor tholeiitic basalt flows.

Based upon field relationships and petrography, Hoffer (1976) divided the alkali-olivine basalts into two members: an older plagioclase-rich member and a younger olivine-rich member. Chemical analysis supported this division showing Member 1 to have a lower MgO concentration than Member 2.

The West Potrillo Basalt flows are interpreted to be the result of the fractional crystallization of a melt of olivine tholeiitic composition, at pressure approaching 13-18 kb and 27 km in depth. The megacrysts are interpreted as being phenocrysts formed in the parental magma as stable phases at high temperature and pressure. The composition of the magma changed only slightly as it rose to the surface as indicated by the only slight reactionof phenocrysts with the host magma. Also, the lack of zoning in the phenocrysts indicate a lack of

compositional change in its route to the surface. This slight change in composition accounts for the small differences in the SI index between Members 1 and 2, which are interpreted to be the result of eruptions from different levels of a differentiating magma chamber. The embayment of the olivine phenocrysts are interpreted to have occurred during the fractionation at depth before mantle diapirism took place.

A P P E N D I X A

BASALT SAMPLE LOCATIONS

APPENDIX A

Sample Locations

201 - Flow, Member 2; NE¼, SW¼, Sec. 35, T26S, R3W.

202 - Flow, Member 1; NW¼, SW¼, Sec. 28, T26S, R3W.

203 - Flow, Member 1; SW¼, NW¼, Sec. 29, T26S, R3W.

204 - Flow, Member 1; NW¼, NW¼, Sec. 33, T26S, R3W.

204A - Feldspar Megacryst; NW¼, NW¼, Sec. 33, T26S, R3W.

205 - Flow, Member 2; NW¼, NW¼, Sec. 32, T26S, R3W.

206 - Flow, Member 2; NE¼, NW¼, Sec. 36, T26S, R4W.

208 - Flow, Member 2; NW¼, SE¼, Sec. 14, T26S, R4W.

209 - Flow, Tholeiitic Basalt; SW¼, SE¼, Sec. 31, T24S, R3W.

210 - Flow, Member 2; NW¼, NW¼, Sec. 21, T25S, R3W.

211 - Flow, Member 2; NE¼, SE¼, Sec. 18, T25S, R3W.

212 - Flow, Member 2; SW¼, SE¼, Sec. 18, T25S, R3W.

213 - Flow, Member 2; SW¼, NW¼, Sec. 20, T25S, R3W.

215 - Flow, Member 2; SW¼, SW¼, Sec. 29, T25S, R3W.

215B,C,D - Feldspar Megacrysts; SW¼, SW¼, Sec. 29, T25S, R3W.

216 - Flow, Member 2; SW¼, SW¼, Sec. 30, T25S, R3W.

APPENDIX A

Sample Locations

216A - Feldspar Megacryst; SE¼, SW¼, Sec. 30, T25S, R3W.

217A,L,M - Feldspar Megacrysts; NE¼, SW¼, Sec. 31, T25S, R3W.

218 - Flow, Member 1; SE¼, SE¼, Sec. 31, T25S, R3W.

218M,N - Feldspar Megacrysts; SE¼, SE¼, Sec. 31, T25S, R3W.

220 - Flow, Member 1; NE¼, NE¼, Sec. 31, T25S, R3W.

221 - Flow, Member 2; NE¼, SW¼, Sec. 29, T25S, R3W.

222 - Flow, Member 2; SE¼, NW¼, Sec. 33, T25S, R3W.

223 - Flow, Member 2; SW¼, NE¼, Sec. 28, T25S, R3W.

226 - Flow, Member 2; NW¼, NE¼, Sec. 34, T24S, R4W.

227 - Volcanic Bomb; SW¼, NE¼, Sec. 34, T24S, R4W.

231 - Flow, Member 2; NE¼, NW¼, Sec. 9, T25S, R3W.

232 - Flow, Member 2; SE¼, SW¼, Sec. 8, T25S, R3W.

233 - Flow, Member 2; SE¼, NW¼, Sec. 8, T25S, R3W.

236 - Volcanic Bomb; SW¼, NW¼, Sec. 33, T24S, R3W.

241 - Flow, Member 2; NW¼, SE¼, Sec. 6, T25S, R3W.

242 - Flow, Tholeiitic Basalt; SE¼, NE¼, Sec. 17, T25S, R3W.

APPENDIX A

Sample Locations

244 - Flow, Member 1; NE¼, SW¼, Sec. 33, T26S, R3W.

246 - Flow, Member 1; SW¼, SE¼, Sec. 27, T26S, R3W.

247 - Flow, Member 1; NE¼, SE¼, Sec. 28, T26S, R3W.

257 - Flow, Member 1; SE¼, NW¼, Sec. 33, T26S, R3W.

258 - Flow, Member 1; SE¼, NE¼, Sec. 32, T26S, R3W.

259 - Flow, Member 1; NE¼, SW¼, Sec. 21, T26S, R3W.

261 - Flow, Member 1; SE¼, NW¼, Sec. 22, T26S, R3W.

270 - Flow, Member 1; SW¼, NE¼, Sec. 15, T25S, R3W.

272A,C,E,K,L - Feldspar Megacrysts; NW¼, NE¼, Sec. 22, T25S, R3W.

273 - Flow, Member 1; SW¼, SE¼, Sec. 22, T25S, R3W.

274A,F,G - Feldspar Megacrysts; NW¼, NE¼, Sec. 27, T25S, R3W.

276A - Feldspar Megacryst; NW¼, SW¼, Sec. 23, T25S, R3W.

282B - Feldspar Megacryst; NE¼, NW¼, Sec. 26, T25S, R3W.

APPENDIX B

POINT COUNTS

APPENDIX B

Point Counts

Member	Sample	Plagioclase	Clinopyroxene	Olivine	Opaque	Glass	Other
1	203	8	16	9	12	46	8 c. 1 Id.
2	205	28	44	9	15	4	0
2	213	17	26	11	17	22	3 C. 4 Un.
2	215	20	35	6	19	20	0
2	216	18	47	12	16	7	0
2	241	21	29	15	15	12	2 Id. 6 An.
1	245	47	20	4	14	15	0
1	246	29	20	9	15	24	2 Id. 1 Un.
1	247	30	24	10	17	18	1 Un.
1	270	24	34	11	13	16	1 Id.

Estimates based on 100 points counted.

An. - Analcime

C. - Calcite

Id. - Iddingsite

Un. - Unknown

A P P E N D I X C

NORM CALCULATIONS

APPENDIX C NORM CALCULATIONS							
SAMPLE ID	Alkali Olivine Basalt	Alkali Olivine Basalt	Basanitoid	Basanitoid	Basanitoid	Tholeiitic Basalt	Basanitoid
SAMPLE #	015	017	018	021	022	024	029
Q	0.0	0.0	0.0	0.0	0.0	0.0	0.0
C	0.0	0.0	0.0	0.0	0.0	0.0	0.0
Or	6.17	5.99	9.41	6.78	7.73	4.03	7.05
Ab	17.86	21.97	7.57	7.04	8.51	25.20	14.84
An	25.47	25.94	20.73	22.63	23.72	24.72	22.08
Lc	0.0	0.0	0.0	0.0	0.0	0.0	0.0
Ne	4.61	1.79	11.01	10.86	9.32	0.0	5.42
Di	20.77	20.00	20.36	32.87	23.05	18.76	23.13
Wo	10.39	10.00	10.18	16.44	11.52	9.38	11.57
En	8.66	8.22	8.86	12.58	8.90	8.05	9.59
Fs	1.73	1.78	1.33	3.86	2.63	1.33	1.98
Hy	0.0	0.0	0.0	0.0	0.0	0.21	0.0
Ol	16.58	14.73	21.91	8.65	18.48	18.97	20.13
Fo	13.82	12.11	19.05	6.62	14.27	16.27	16.68
Fa	2.76	2.62	2.85	2.03	4.21	2.70	3.44
Mt	4.02	4.44	4.22	5.01	4.31	3.89	3.58
Il	3.26	3.77	3.54	4.53	3.64	3.09	2.67
Ap	1.26	1.37	1.25	1.63	1.24	1.14	1.10
Cc	0.0	0.0	0.0	0.0	0.0	0.0	0.0
TTI*	27.0	28.1	26.3	22.3	23.6	27.9	25.9

* Thornton-Tuttle Index

APPENDIX C NORM CALCULATIONS

SAMPLE ID	Basanitoid	Alkali Olivine Basalt	Basanitoid	Alkali Olivine Basalt	Basanitoid	Basanitoid	Tholeiitic Basalt
SAMPLE #	033	037	038	043	045	047	050
Q	0.0	0.0	0.0	0.0	0.0	0.0	0.0
C	0.0	0.0	0.0	0.0	0.0	0.0	0.0
Or	8.92	9.78	9.07	9.91	10.55	8.29	5.54
Ab	12.91	16.92	10.00	18.73	14.02	11.71	24.82
An	24.32	21.29	22.54	24.22	22.79	19.65	25.52
Lc	0.0	0.0	0.0	0.0	0.0	0.0	0.0
Ne	6.81	4.90	8.63	4.11	6.48	7.67	0.0
Di	19.55	16.20	22.20	18.24	19.27	25.47	16.33
Wo	9.77	8.10	11.09	9.12	9.64	12.73	8.16
En	7.76	6.81	8.92	7.37	7.58	10.57	6.20
Fs	2.01	1.29	2.17	1.75	2.06	2.17	1.97
Hy	0.0	0.0	0.0	0.0	0.0	0.0	7.24
Ol	20.19	22.15	17.51	14.92	17.68	18.88	10.96
Fo	16.04	18.61	14.09	12.05	13.91	15.67	8.32
Fa	4.15	3.54	3.43	2.87	3.77	3.21	2.64
Mt	3.55	4.12	4.57	4.52	4.20	3.82	4.31
Il	2.63	3.41	3.97	3.91	3.49	2.99	3.61
Ap	1.12	1.23	1.53	1.45	1.52	1.51	1.68
Cc	0.0	0.0	0.0	0.0	0.0	0.0	0.0
TTI*	27.1	30.2	25.7	30.9	29.2	26.0	28.6

* Thornton-Tuttle Index

APPENDIX C NORM CALCULATIONS

SAMPLE ID	Alkali Olivine Basalt	Alkali Olivine Basalt	Alkali Olivine Basalt	Alkali Olivine Basalt	Alkali Olivine Basalt	Basanitoid	Basanite
SAMPLE #	052	053	060	061	063	065	066
Q	0.0	0.0	0.0	0.0	0.0	0.0	0.0
C	0.0	0.0	0.0	0.0	0.0	0.0	0.0
Or	9.89	7.92	10.00	10.16	4.62	9.83	7.69
Ab	18.48	23.33	20.92	15.48	21.75	12.68	0.0
An	23.27	25.14	23.91	26.60	20.12	27.37	20.40
Lc	0.0	0.0	0.0	0.0	0.0	0.0	0.29
Ne	3.80	0.89	2.37	2.74	3.74	6.85	15.08
Di	16.46	15.12	15.96	13.62	17.46	19.36	37.18
Wo	8.23	7.56	7.98	6.81	8.73	9.69	18.59
En	6.51	5.66	6.22	5.78	7.72	7.86	14.31
Fs	1.72	1.90	1.76	1.03	1.01	1.84	4.28
Hy	0.0	0.0	0.0	0.0	0.0	0.0	0.0
Ol	19.24	20.07	18.10	23.39	23.42	14.33	9.68
Fo	15.22	15.02	14.11	19.83	20.72	11.62	7.45
Fa	4.02	5.05	3.99	3.55	2.70	2.72	2.23
Mt	4.15	3.65	4.10	3.88	4.24	4.43	4.48
Il	3.43	2.75	3.35	3.07	3.58	3.79	3.84
Ap	1.28	1.13	1.28	1.06	1.07	1.33	1.36
Cc	0.0	0.0	0.0	0.0	0.0	0.0	0.0
TTI*	30.5	30.7	31.7	27.3	28.7	27.5	20.6

* Thornton-Tuttle Index

APPENDIX C NORM CALCULATIONS

SAMPLE ID	Alkali Olivine Basalt	Basanitoid	Basanite	Alkali Olivine Basalt	Alkali Olivine Basalt	Tholeiitic Basalt	Basanitoid
SAMPLE #	067	070	072	073	074	075	076
Q	0.0	0.0	0.0	0.0	0.0	0.0	0.0
C	0.0	0.0	0.0	0.0	0.0	0.0	0.0
Or	7.62	8.59	5.26	8.63	12.25	10.27	7.89
Ab	21.13	15.30	0.0	16.44	22.91	24.41	11.86
An	25.35	22.71	21.57	24.74	23.43	24.58	25.73
Lc	0.0	0.0	3.59	0.0	0.0	0.0	0.0
Ne	1.99	8.17	14.25	4.95	1.17	0.0	7.06
Di	17.14	20.32	38.67	18.99	12.95	10.64	19.25
Wo	8.57	10.16	19.33	9.50	6.47	5.32	9.63
En	6.53	8.27	14.64	7.58	4.94	4.14	7.66
Fs	2.04	1.89	4.69	1.91	1.53	1.18	1.97
Hy	0.0	0.0	0.0	0.0	0.0	1.16	0.0
Ol	17.98	16.00	8.98	15.86	17.65	22.09	20.52
Fo	13.69	13.02	6.80	12.66	13.47	17.20	16.32
Fa	4.29	2.98	2.18	3.20	4.18	4.89	4.20
Mt	3.97	4.44	3.53	4.76	4.56	3.30	3.63
Il	3.19	3.82	2.61	4.23	3.94	2.31	2.75
Ap	1.62	1.16	1.56	1.39	1.16	1.23	1.31
Cc	0.0	0.0	0.0	0.0	0.0	0.0	0.0
TTI*	29.1	30.0	20.8	28.2	34.5	33.5	25.3

* Thornton-Tuttle Index

APPENDIX C NORM CALCULATIONS

SAMPLE ID	Basanitoid	Basanitoid	Basanitoid	Basanite	Alkali Olivine Basalt	Tholeiitic Basalt	Alkali Olivine Basalt
SAMPLE #	077	078	081	082	083	084	085
Q	0.0	0.0	0.0	0.0	0.0	0.0	0.0
C	0.0	0.0	0.0	0.0	0.0	0.0	0.0
Or	8.36	12.60	9.22	7.75	7.56	4.47	5.58
Ab	12.04	15.75	13.08	9.48	17.50	25.45	24.97
An	23.92	18.59	22.81	22.71	23.39	23.47	23.65
Lc	0.0	0.0	0.0	0.0	0.0	0.0	0.0
Ne	6.96	8.76	7.28	12.43	4.89	0.0	0.84
Di	19.98	18.40	22.30	29.16	22.74	19.27	20.26
Wo	9.99	9.20	11.15	14.58	11.37	9.63	10.13
En	8.31	7.32	8.94	9.54	8.37	7.55	8.27
Fs	1.68	1.88	2.21	5.04	3.00	2.08	1.86
Hy	0.0	0.0	0.0	0.0	0.0	9.82	0.0
Ol	20.27	17.45	15.19	8.76	15.37	9.07	15.73
Fo	16.87	13.89	12.18	5.73	11.32	7.11	12.86
Fa	3.40	3.56	3.01	3.03	4.06	1.96	2.88
Mt	4.08	4.02	4.65	4.52	3.99	3.94	4.28
Il	3.35	3.25	4.08	3.88	3.20	3.15	3.60
Ap	1.04	1.18	1.39	1.31	1.35	1.36	1.08
Cc	0.0	0.0	0.0	0.0	0.0	0.0	0.0
TTI*	25.8	35.1	27.6	26.8	28.0	28.8	29.8

* Thornton-Tuttle Index

APPENDIX C NORM CALCULATIONS

SAMPLE ID	Alkali Olivine Basalt	Alkali Olivine Basalt	Alkali Olivine Basalt	Alkali Olivine Basalt	Alkali Olivine Basalt	Basanitoid	Basanitoid
SAMPLE #	088	088A	095	097	102	103	104
Q	0.0	0.0	0.0	0.0	0.0	0.0	0.0
C	0.0	0.0	0.0	0.0	0.0	0.0	0.0
Or	11.13	13.22	9.34	6.96	10.35	8.68	9.26
Ab	23.25	22.48	21.85	23.21	20.97	12.51	9.64
An	25.55	19.27	24.56	25.12	21.07	27.04	27.01
Lc	0.0	0.0	0.0	0.0	0.0	0.0	0.0
Ne	0.98	2.79	1.71	1.51	3.28	7.62	9.41
Di	10.01	13.46	13.17	21.47	16.20	23.79	22.88
Wo	5.00	6.73	6.59	10.74	8.10	11.89	11.44
En	3.70	5.20	5.17	7.69	6.04	8.80	8.31
Fs	1.31	1.53	1.41	3.04	2.06	3.09	3.13
Hy	0.0	0.0	0.0	0.0	0.0	0.0	0.0
Ol	20.23	20.64	21.00	11.17	19.24	11.61	12.58
Fo	14.94	15.94	16.49	8.00	14.36	8.60	9.14
Fa	5.28	4.70	4.51	3.17	4.89	3.02	3.44
Mt	4.07	3.87	3.89	4.83	4.16	4.11	4.33
Il	3.29	3.06	3.09	4.28	3.41	3.36	3.65
Ap	1.50	1.20	1.39	1.44	1.32	1.27	1.24
Cc	0.0	0.0	0.0	0.0	0.0	0.0	0.0
TTI*	33.7	36.9	31.4	29.6	32.8	26.7	26.1

* Thornton-Tuttle Index

APPENDIX C NORM CALCULATIONS

SAMPLE ID	Basanitoid	Alkali Olivine Basalt	Alkali Olivine Basalt	Basanitoid	Basanitoid	Basanitoid	Basanitoid
SAMPLE #	105	201	202	203	204	205	206
Q	0.0	0.0	0.0	0.0	0.0	0.0	0.0
C	0.0	0.0	0.0	0.0	0.0	0.0	0.0
Or	9.02	5.70	9.17	3.87	10.32	8.40	8.48
Ab	13.24	23.88	20.57	13.06	13.31	12.47	12.19
An	22.62	22.26	21.39	19.23	19.89	18.33	19.20
Lc	0.0	0.0	0.0	0.0	0.0	0.0	0.0
Ne	6.65	1.64	3.25	7.80	7.54	8.17	8.69
Di	22.68	18.03	17.18	32.03	21.99	23.30	20.45
Wo	11.34	9.01	8.59	16.01	11.00	11.65	10.22
En	8.69	7.31	7.02	12.30	8.94	9.50	8.79
Fs	2.65	1.70	1.57	3.72	2.05	2.15	1.43
Hy	0.0	0.0	0.0	0.0	0.0	0.0	0.0
Ol	17.00	20.47	18.90	15.67	17.53	20.84	22.21
Fo	13.03	16.61	15.45	12.03	14.26	16.99	19.10
Fa	3.97	3.86	3.46	3.64	3.27	3.85	3.10
Mt	4.06	3.88	4.40	3.96	4.31	4.01	4.13
Il	3.28	3.07	3.75	3.17	3.64	3.23	3.43
Ap	1.46	1.08	1.38	1.21	1.46	1.25	1.22
Cc	0.0	0.0	0.0	0.0	0.0	0.0	0.0
TTI*	27.0	29.8	31.3	22.8	29.3	27.3	27.7

* Thornton-Tuttle Index

APPENDIX C NORM CALCULATIONS							
SAMPLE ID	Alkali Olivine Basalt	Tholeiitic Basalt	Basanitoid	Alkali Olivine Basalt	Basanitoid	Basanitoid	Basanitoid
SAMPLE #	208	209	210	211	212	213	215
Q	0.0	5.07	0.0	0.0	0.0	0.0	0.0
C	0.0	0.0	0.0	0.0	0.0	0.0	0.0
Or	4.49	8.45	9.97	10.85	9.46	10.12	8.15
Ab	21.88	27.92	16.28	17.45	10.48	15.03	14.02
An	20.48	23.15	20.66	22.02	19.93	20.29	21.67
Lc	0.0	0.0	0.0	0.0	0.0	0.0	0.0
Ne	2.88	0.0	5.83	4.94	9.02	6.44	6.24
Di	19.11	10.95	17.79	15.79	20.29	18.34	18.31
Wo	9.55	5.47	8.90	7.90	10.15	9.17	9.16
En	8.34	3.32	7.32	6.18	8.44	7.40	7.72
Fs	1.22	2.15	1.58	1.71	1.71	1.77	1.44
Hy	0.0	16.53	0.0	0.0	0.0	0.0	0.0
Ol	21.92	0.0	20.28	19.60	22.14	20.72	23.08
Fo	19.13	0.0	16.68	15.35	18.42	16.72	19.45
Fa	2.79	0.0	3.60	4.25	3.72	4.00	3.63
Mt	4.30	3.97	4.27	4.31	4.08	4.24	4.08
Il	3.64	3.14	3.58	3.62	3.35	3.53	3.34
Ap	1.31	0.83	1.34	1.41	1.24	1.29	1.10
Cc	0.0	0.0	0.0	0.0	0.0	0.0	0.0
TTI*	27.8	39.39	30.4	31.5	27.3	29.9	27.0

* Thornton-Tuttle Index

APPENDIX C NORM CALCULATIONS							
SAMPLE ID	Basanitoid	Basanitoid	Alkali Olivine Basalt	Basanitoid	Alkali Olivine Basalt	Alkali Olivine Basalt	Alkali Olivine Basalt
SAMPLE #	216	218	220	221	222	223	226
Q	0.0	0.0	0.0	0.0	0.0	0.0	0.0
C	0.0	0.0	0.0	0.0	0.0	0.0	0.0
Or	8.58	9.90	12.08	7.07	6.66	10.21	3.60
Ab	12.13	11.20	23.09	15.42	21.75	19.14	19.54
An	18.84	19.76	21.24	20.38	22.49	21.62	21.87
Lc	0.0	0.0	0.0	0.0	0.0	0.0	0.0
Ne	8.10	9.17	1.73	6.44	2.43	4.26	3.08
Di	20.00	25.68	15.51	18.83	17.17	15.69	22.55
Wo	10.00	12.84	7.75	9.42	8.59	7.84	11.27
En	8.60	9.89	5.64	8.04	7.13	6.21	9.41
Fs	1.40	2.95	2.11	1.37	1.45	1.63	1.86
Hy	0.0	0.0	0.0	0.0	0.0	0.0	0.0
Ol	24.19	16.15	17.46	22.98	21.09	20.03	21.92
Fo	20.81	12.44	12.71	19.62	17.52	15.86	18.30
Fa	3.38	3.71	4.75	3.35	3.57	4.16	3.62
Mt	3.89	3.83	4.18	4.13	4.05	4.24	3.67
Il	3.10	3.00	3.43	3.42	3.31	3.34	2.80
Ap	1.17	1.32	1.28	1.33	1.06	1.27	0.98
Cc	0.0	0.0	0.0	0.0	0.0	0.0	0.0
TTI*	27.4	28.3	35.0	27.4	29.4	31.9	24.9

* Thornton-Tuttle Index

APPENDIX C NORM CALCULATIONS							
SAMPLE ID	Basanitoid	Alkali Olivine Basalt	Alkali Olivine Basalt	Basanitoid	Tholeiitic Basalt	Alkali Olivine Basalt	Tholeiitic Basalt
SAMPLE #	231	232	233	241	242	244	246
Q	0.0	0.0	0.0	0.0	6.14	0.0	0.0
C	0.0	0.0	0.0	0.0	0.0	0.0	0.0
Or	10.31	11.16	11.22	9.74	9.17	7.80	6.56
Ab	16.64	24.71	23.06	9.32	29.25	26.96	26.61
An	20.12	21.55	20.33	19.54	20.48	20.32	23.49
Lc	0.0	0.0	0.0	0.0	0.0	0.0	0.0
Ne	6.02	0.86	2.47	9.94	0.0	2.14	0.0
Di	16.75	13.26	14.10	23.94	9.0	22.63	15.58
Wo	8.38	6.63	7.05	11.97	4.50	11.31	7.79
En	6.79	4.99	5.38	9.50	3.32	7.54	6.18
Fs	1.58	1.64	1.67	2.47	1.18	3.77	1.61
Hy	0.0	0.0	0.0	0.0	18.04	0.0	0.91
Ol	21.28	19.25	19.81	18.75	0.0	11.80	17.01
Fo	17.26	14.48	15.12	14.88	0.0	7.87	13.50
Fa	4.02	4.77	4.68	3.87	0.0	3.93	3.51
Mt	4.12	4.24	4.16	4.11	3.91	3.92	4.52
Il	3.40	3.52	3.42	3.37	3.07	3.08	3.90
Ap	1.38	1.44	1.43	1.29	0.94	1.34	1.42
Cc	0.0	0.0	0.0	0.0	0.0	0.0	0.0
TTI*	31.3	35.0	35.0	27.1	42.8	34.6	31.5

* Thornton-Tuttle Index

APPENDIX C NORM CALCULATIONS

SAMPLE ID	Tholeiitic Basalt	Tholeiitic Basalt	Alkali Olivine Basalt	Alkali Olivine Basalt	Alkali Olivine Basalt	Alkali Olivine Basalt	Basanitoid
SAMPLE #	247	257	258	259	261	270	273
Q	0.0	0.0	0.0	0.0	0.0	0.0	0.0
C	0.0	0.0	0.0	0.0	0.0	0.0	0.0
Or	6.28	7.99	7.88	7.53	7.48	11.00	8.98
Ab	26.89	26.27	24.47	24.21	24.73	22.32	9.95
An	23.14	23.62	22.75	22.78	23.32	20.84	20.13
Lc	0.0	0.0	0.0	0.0	0.0	0.0	0.0
Ne	0.0	0.0	1.01	1.17	0.81	2.64	8.86
Di	16.54	14.18	16.58	16.51	14.71	15.71	28.76
Wo	8.27	7.09	8.29	8.26	7.36	7.86	14.38
En	6.45	5.74	6.58	6.69	6.14	5.85	10.99
Fs	1.82	1.35	1.71	1.56	1.22	2.01	3.39
Hy	0.85	1.76	0.0	0.0	0.0	0.0	0.0
Ol	16.48	16.24	17.46	18.16	19.25	19.35	16.28
Fo	12.85	13.16	13.86	14.72	16.06	14.40	12.44
Fa	3.63	3.08	3.61	3.44	3.18	4.95	3.84
Mt	4.50	4.52	4.52	4.46	4.49	3.82	3.37
Il	3.86	3.92	3.90	3.83	3.88	2.98	2.40
Ap	1.46	1.50	1.42	1.33	1.34	1.33	1.28
Cc	0.0	0.0	0.0	0.0	0.0	0.0	0.0
TTI*	31.4	32.6	31.6	31.3	31.5	34.3	26.0

* Thornton-Tuttle Index

A P P E N D I X D

DESCRIPTION OF FELDSPAR SAMPLES

APPENDIX D

Description of Feldspar Megacrysts

SAMPLE	SIZE(cm)	WEIGHT(g)	COMMENTS
204A	3x2x1	9.7	clear,pitted,no twinning
215B	2x1x1	3.9	clear,fine twinning
215C	2½x1x1	4.2	white,fine twin
215D	3x2½x2	19.6	subrounded,pitted,fe stain
216A	2x1x1½	6.2	white,fe stain
217A	3x2x2	13.9	white,pitted
217L	3x2x1½	12.1	subrounded,pitted,clear
217M	3x1½x1	5.8	clear,fine to coarse twin
218M	3x1x1	5.1	white,fe stain,no twinning
218N	2x1½x1	4.5	grey
272A	2x2x½	2.9	clear,no twin
272C	2½x1x1	5.2	clear
272E	3x1x1	5.1	clear,pitted
272K	3½x3½x2	23.1	subrounded,pitted,fe stain white

APPENDIX D
(con't)

SAMPLE-	SIZE(cm)	WEIGHT(g)	COMMENTS
272L	2x1½x1	4.7	white,pitted
274A	2x2x1½	5.1	clear,no twin,fe stain
274F	2½x2x1	10.4	clear
274G	3x1½x1	10.9	clear,fe stain,no twin
276A	3x2x1	9.6	white,pitted,coarse twin
282B	2x1x1	3.2	white,pitted,no twin

REFERENCES

Baldridge, W. S.,1979, Petrology and petrogenesis of Plio-Pleistocene basaltic rocks from the central Rio Grande rift, Rio Grande Rift: Tectonics and Magmatism, Robert E. Riecker edition, p. 323-353.

Bersch, M.G.,1977, Petrography and Geology of the Southern West Potrillo Basalt Field, Dona Ana County, New Mexico, unpub. Masters thesis, Univ. Texas at El Paso, 60p.

Binns, R.A., Ouggan, M.B., and Wilkinson, J.F.G.,1970, High Pressure Megacrysts in alkaline lavas from north-eastern New South Wales: Am. J. Sci., v. 269, p. 132-168.

Bultitude, R.J., and Green, D.H.,1968, Experimental study at high pressures on the origin of olivine nephelinite and olivine melilite nephelinite magmas, Earth Planet Sci. Letters 3, p. 325-337.

Carmichael, J.S.E., Turner, F.J., and Verhoogan, J.,1974, Igneous Petrology, McGraw-Hill Book Company.

Chapin, C.E.,1979, Evolution of the Rio Grande rift-a summary in Rio Grande Rift: Tectonics and Magmatism, Robert E. Rieker, ed.: Am. Geophys. Union spec. pub., p.195-208.

Chapin, C.E., and Seager, W.R.,1975, Evolution of Rio Grande rift in the Socorro and Las Cruces areas: New Mexico Geol. Soc. Guidebook 26th Field Conf., Las Cruces country, p. 297-322.

Cox, K.G., Bell, J.D., and Pankhurst, R.J.,1979, The Interpretation of Igneous Rocks, George Allen and Unwin LTD.

DeHon, R.A.,1965, Maare of La Mesa: New Mexico Geol. Soc. Guidebook 16th Field Conf., Southwestern New Mexico II, p. 204-209.

Fenneman, N.M.,1931, Physiography of the Western United States, McGraw-Hill, Inc., New York, 534p.

Hawley, J., and Kottlowski, F.E.,1969, Quaternary geology of the southcentral New Mexico border region in Border stratigraphy Symposium, F.E. Kottlowski and D.V. LaMone (eds.), New Mexico Bur. Mines and Min. Res., Circ. 104, p. 89-104.

Hoffer, J.M.,1969, Volcanic history of the Black Mountain-Santo Tomas basalts, Potrillo volcanics, Dona Ana County, New Mexico, in Guidebook of the Border Region: N. Mex. Geol. Soc., Guidebook, 20th Field Conf., p. 108-114.

_____,1973, Quaternary basalts of the West Potrillo Mountains, south-central NewMexico. El Paso Geol. Soc. Guidebook 7, p. 26-32.

_____,1976, Geology of Potrillo Basalt Field, South-central New Mexico, New Mex. Bur. Mines and Min. Res., Circ. 149, 30p.

Hoffer, J.M., and Hoffer, R.L.,1973, Composition and structural state of feldspar inclusions from alkali olivine basalt, Potrillo Basalt, southern New Mexico, G.S.A. Bull., v. 84, p. 2139-2142.

Irvine, T.N., and Barager, W.R.A.,1971, A guide to the chemical classification of the common volcanic rocks. Canadian Jour. of Earth Sci., v. 8, p. 523-548.

King, W.E., Hawley, J.W., Taylor, A.M., and Wilson, R.P., 1969, Hydrogeology of the Rio Grande valley and adjacent intermontane areas of southern New Mexico: Water Resources Inst., Rept. 6, New Mexico State Univ., 141p.

Kuno, H.,1968, Differentiation in basalt magmas, in Basalts: the Poldervaart treatise on rocks of basaltic composition: Interscience Publishers, New York, 862 p.

Kuno, H., Yamasaki, K., Iida, C., and Nagashima, K.,1957, Differentiation of Hawaiian magmas: Japanese Jour. Geology Geography, v. 28, 179-218.

Laughlin, A.W., Manzer, G.K., Jr., and Carden, J.R.,1974, Feldspar megacrysts in alkali basalts, G.S.A. Bull., v. 85, p. 413-416.

Millican, R.S., 1971, Geology and petrography of the Tertiary Mt. Riley-Cox pluton, Dona Ana County, New Mexico, M.S. thesis, Univ. of Texas at El Paso 87p.

Muir, I.D., and Tilley, C.E.,1961, Mugearites and their place in alkaline igneous rocks series: J. Geol., v. 69, p. 186-203.

C - 2

Ortiz, T.S.,1979, Megacrysts and Mafic and Ultramafic inclusions of the Southern West Potrillo Basalt Field, Dona Ana County, New Mexico, unpub. Masters thesis, Univ. Texas at El Paso, 95p.

Pearce, J.A.,1976, Statistical Analysis of Major Element Patterns in Basalts, J. Petrology,19,p. 66-94.

Renault, J.R., Major-element variations in the Potrillo, Carrizozo, and McCartys basalt fields, New Mexico: New Mexico Bur. Mines Mineral Resources, Circ. 113, 22p.

Ringwood, A.E., Composition and petrology of the earths mantle, McGraw-Hill, New York, 618 p., 1975.

Seager, W.R., and Morgan, P.,1979, Rio Grande rift in southern New Mexico, West Texas, and Magmatism, Robert E. Reicker, ed.: Am. Geoph. Union Spec. Pub., p. 87-106.

Thornton, C.P., and Tuttle, O.F., 1960, Chemistry of Igneous Rocks I. Differentiation Index, Amer. Jour. Sci., v. 258, p. 661-684.

U.S. Department of Agriculture, Climate and man: p. 1012,1941.

Warren, R.G., Kudo, A.M., and Keil, K.,1979, Geochemistry of lithic and single crystal inclusions in basalt and a characterization of the upper mantle-lower crust in the Engle Basin, Rio Grande rift, New Mexico in Rio Grande Rift: Tectonics and Magmatism, Robert E. Reicker, ed.: Am. Geoph. Union spec. pub., p. 393-415.

Wilshire, H.G., and Pike, J.E.N.,1975, Upper mantle diapirism: Evidence from analogous features in alpine peridotite and ultramafic inclusions in basalt, Geol., v. 3, p. 467-470.

Yoder, H.S.,1973, Contemporaneous Basaltic and Rhyolitic Magmas, Amer. Min., 58, p. 153-171.

VITA

Tatum M. Sheffiled was born in [redacted], [redacted], the son of Rufus and Ovon Sheffield. After graduating from Nederland High School in Nederland, Texas, he entered Lamar University at Beaumont, Texas. He received the Bachelor of Science degree in August of 1978. In the fall of 1979, he entered the Graduate School of the University of Texas at El Paso.

This thesis was typed by Ms. Sandy Ladewig.